1-1-2013

# Numerical Analysis of Film Cooling from Micro-Hole

Silambarasan Balasubrammaniyan
*Ryerson University*

# NUMERICAL ANALYSIS OF FILM COOLING FROM MICRO-HOLE

By

Silambarasan Balasubramaniyan, B.E

Aeronautical Engineering

Anna University

A project presented to Ryerson University

In Partial fulfillment of the requirements for the degree of

Master of Engineering

In the Program of

Aerospace Engineering

Toronto, Ontario, Canada, 2013

## Author’s Declaration

AUTHOR'S DECLARATION FOR ELECTRONIC SUBMISSION OF A THESIS

I hereby declare that I am the sole author of this thesis. This is a true copy of the thesis, including any required final revisions, as accepted by my examiners.

I authorize Ryerson University to lend this thesis to other institutions or individuals for the purpose of scholarly research

I further authorize Ryerson University to reproduce this thesis by photocopying or by other means, in total or in part, at the request of other institutions or individuals for the purpose of scholarly research.

I understand that my thesis may be made electronically available to the public.

## Abstract

The performance of aircraft gas turbine engines mainly depends on performance of the turbine which expands the combusted air into the atmosphere. The turbine is a critical part which gets affected by the hot gas from combustor exhaust. So in order to enhance the performance of gas turbine engines, a proposed cooling type called film cooling is used for more than six decades. The current work is also an attempt to enhance the performance of the gas turbine engine by enhancing the film cooling performance. The film cooling performance was numerically calculated on a flat plate with micro-hole and compared the cooling performance from the macro-hole. The analysis was carried out for different blowing ratios and found that the coolant from micro-hole performs better in the vicinity region and also spreads well in the lateral direction. The vortex structure is also captured from the proposed turbulence model and discussed. The behaviour of micro flow inside the coolant pipe was also analyzed. The comparison between multiple micro-hole jets and discrete jets was also made and discussed.

## Acknowledgements

I would like to thank my supervisor Dr. Bassam Ali Jubran for introducing me into the world of film cooling and CFD. The courses he suggested enhanced my knowledge on fluid mechanics, gas turbine engines and basics on CFD. I would also like to thank him for his patience while responding my mail and answering my questions.

I would also like to thank Dr.Hartmut Schmider and Mr. Siavash Khajehhasani for their guidance in HPCVL, GAMBIT and FLUENT.

I would like to thank my friends from the program especially Partha, Hemachandran and others for their support and encouragement.

Last, but not least I need to be grateful to my parents and family members for their sacrifice and the tremendous efforts for bringing me up to this stage.

# Table of Contents

# Nomenclature

| | |
|---|---|
| D | Diameter of the Hole |
| M | Blowing Ratio |
| L | Length of the Coolant hole |
| L/D | Length over Diameter ratio |
| P/D | Pitch over Diameter ratio |
| $\eta$ | Effectiveness of film cooling |
| $\overline{\eta}$ | Laterally averaged effectiveness of film cooling |
| $\rho_c$ | Density of the coolant |
| $\rho_g$ | Density of the hot gas |
| $T_c$ | Temperature of the coolant |
| $T_g$ | Temperature of the hot gas |
| $T_{aw}$ | Adiabatic temperature of the wall |
| $U_c$ | Velocity of the coolant |
| $U_g$ | Velocity of the hot gas |
| RKE | Realizable K-ε turbulence model |
| SKE | Standard K-ε turbulence model |
| S-A | Spalart-Allmaras turbulence model |
| MTJ | Micro-Tangential Jet[21] |

# List of Tables



# List of Figures

# Chapter 1: Introduction to Film Cooling

## 1.1 Turbine Cooling

Gas turbine engines are an integral part of the aerospace industries. The jet engines works according to the Brayton cycle as shown in Fig.1, where air enters through the inlet (stage 0), its temperature gets increased due to compression in the compressor (stage 0-2), the temperature of compressed air reaches its peak level due to the addition of fuel in the combustion chamber (stage 2-3), the high temperature gas then expands with the help of the turbine and is expelled to the atmosphere through the nozzle (stage 3-4).

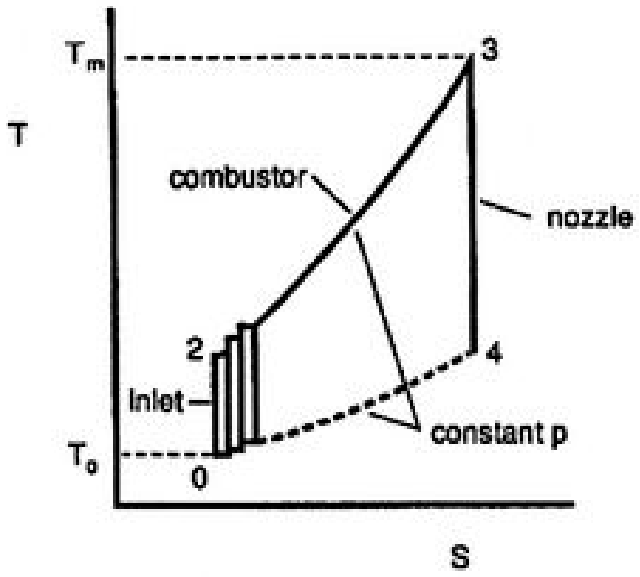


**Fig. 1 BraytonCycle** [23]

Thermal efficiency and power output of the gas turbine engines depends on the Turbine Inlet Temperature (TIT). Over the decades researchers focused on improving the performance of gas turbine engines by increasing TIT. Increasing TIT could lead to failure of turbine blade material. Fig.2 [1] shows the involvement of cooling scheme in the increase of TIT from 1200K to 2400K for the past six decades. The selection of cooling scheme differs from manufacturer to manufacturer, and though transpiration cooling gives better performance film cooling was the most widely applied cooling scheme**.**

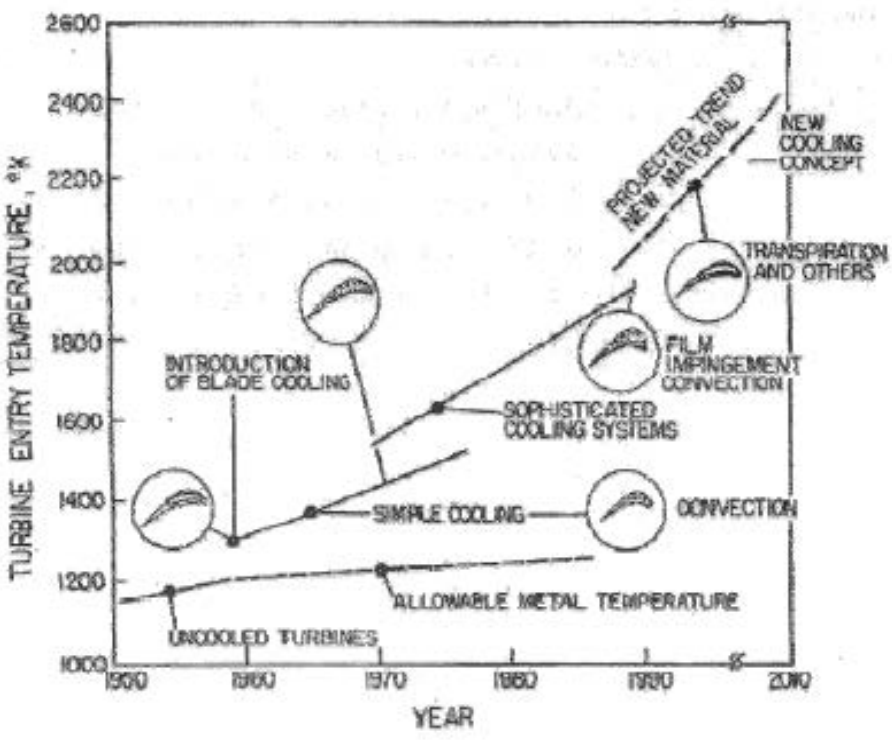


**Fig. 2 Variation of turbine entry temperature with different cooling technique [1]**

Transpiration cooling is the one which provides better cooling performance as shown in Fig.2 [1]. The coolant is ejected through the porous wall of the blade material which thickens the oncoming mainstream flow boundary layer to increase the cooling performance. The disadvantage on transpiration cooling is its difficulty in maintaining the porosity of the holes and aerodynamic loss due to the normal injection of the coolant from the porous wall. Slot cooling was the one among the other cooling scheme which delivered better cooling performance but this is also not used by many manufacturers due to material integrity.

Film cooling provides lesser cooling performance than transpiration cooling and is the widely applied cooling scheme by the aircraft turbine engine manufacturers. The coolant air is bleed from the compressor and is injected in to the heated surface, which indirectly causes a penalty in the reduction in thermal efficiency of the engine. Reduction on the amount of coolant used for cooling purpose compensates the loss in thermal efficiency. Researchers on film cooling focused on reducing the mass flow of coolant by reducing the area of the coolant hole. The current paper also focuses on achieving better film cooling performance by using a lesser amount of coolant with the help of micro-hole.

### 1.2 Film Cooling

The coolant air introduced at certain locations form a protective thermal barrier over the surface to be cooled [1]. In gas turbine engine the coolant air from the compressor enters through the root of the blade, ejected at discrete location through film cooling holes and forms a blanket of coolant on the surface of the blade.

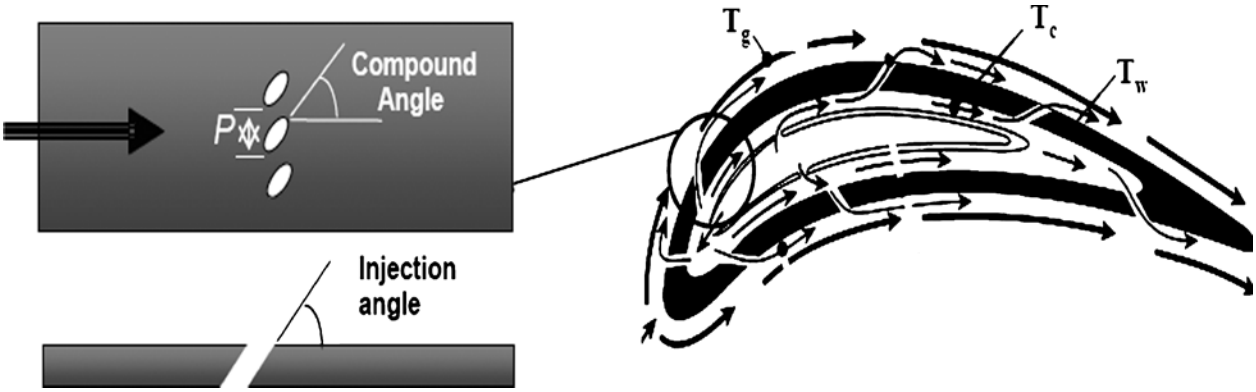


**Fig. 3 Typical location of film cooling holes in turbine blade [2]**

The Fig 3 [2] shows the typical locations of film cooling holes on turbine blade, where the hot gas temperature was denoted as $T_g$, coolant temperature as $T_c$ and the adiabatic wall temperature as $T_{aw}$. The film cooling performance is calculated in-terms of a non-dimensional temperature term defined as the adiabatic effectiveness (η)

$$\eta = \frac{T_g - T_{aw}}{T_g - T_c} \qquad (1)$$

The maximum effectiveness occurs when η=1 and variation in η indicates the film cooling performance. The adiabatic effectiveness can be affected by various mainstream and geometrical parameters as shown in Table.1

**Table 1 Factors affecting film cooling performance**

| Coolant/Mainstream Conditions | Hole Geometry and Configuration |
|---|---|
| Mass & Momentum Flux Ratio | Shape of the Hole |
| Density Ratio | Length of the Hole (L) |
| Mainstream Turbulence | Injection Angle |

Researchers over the six decades have focused to improve the adiabatic film cooling effectiveness by varying the parameters and configuration as mentioned above.

### 1.2.1 Flow structure

The coolant jet penetration into mainstream flow is complex in nature. Coolant jet released from the coolant hole gets deflected by the mainstream flow and the flow spreads laterally downstream. The shear in the cross flow causes coolant to spread laterally in downstream direction of the hole. The structure is strongly three dimensional in nature as shown in Fig 4 [6] and has four vortical structures that have been studied by many researchers experimentally and numerically.

Thole et al [3] experimentally studied the effect of the velocity profile of coolant in hole by varied the flow direction and velocity in the plenum. Andreopoulos et al [4] observed the counter rotating kidney shaped vortices far away from the exit of the hole. Zhou [6] observed that the strong residual vortices within boundary layer cancelled the circulation of primary vortex rings that emerged from the coolant hole, and resulted in hairpin vortices at the low velocity ratio. But, at high velocity ratio the strong emerging vortices overcomes the effect of residual vortices and results in tilted vortices. Walters and Leylek [8] followed a Novel Vorticity based approach and compared their computational result with experimental results and also highlighted the complex flow structure with all features and identified the source for counter rotating vortices. Ligrani et al [22] reported that the vortex generated during jet lift off pulls the hot mainstream air towards the coolant surface to result in low performance of film cooling.

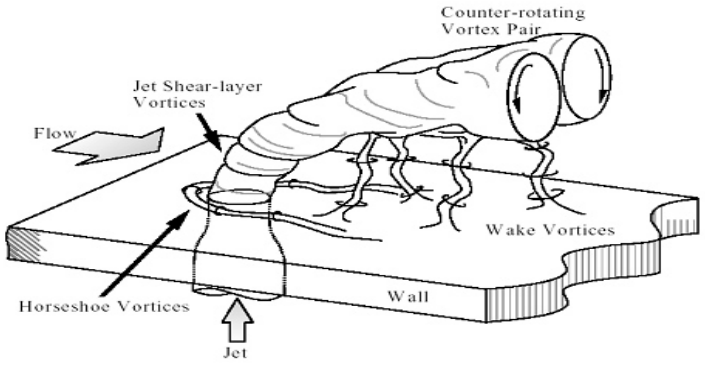


**Fig. 4 Complex cross flow structure [6]**

The boundary layer formed in the mainstream flow was observed at leading edge of the coolant hole and a new boundary layer was developed downstream of coolant hole. The jet shear layer vortices in Fig.4 [6] are coherent in structures formed at the exit of coolant hole. The

horseshoe vortices induced by the emerging jet shear layer vortices wrap around the jet efflux from the hole and cause the coolant to lift away from wall. At low blowing ratio, the horseshoe vortices disappear before a new jet shear-layer vortex emerges from hole and causes coolant to attach with the wall, and vice versa for high velocity ratio. The wake vortices are formed in downstream region of the coolant hole, which is in the immediate vicinity region of coolant hole and in mainstream flow direction.

### 1.2.2 Parameters affecting Film cooling Performance

Film cooling performance mainly depends on the parameters mentioned in the Table 1. A sufficient amount of research has been done on various parameters and only few have been discussed in this section.

1. Blowing Ratio(M):

The ratio of the mass flux of coolant and mainstream flow is defined as blowing ratio (M) and is numerically defined as follows

$$\mathbf{M} = \frac{\rho_c U_c}{\rho_g U_g} \tag{2}$$

Where $\rho_c$ and $U_c$ are the coolant properties and $\rho_g$ and $U_g$ are the hot mainstream gas properties respectively. The change in M has a tremendous effect on film cooling performance. Bogard and Thole [2] mentioned that the effectiveness was maximum at M=0.6 and for M ≥ 0.85 the position of maximum effectiveness moves downstream. The decrease in effectiveness indicates the coolant jet separation from the surface and reattachment at a certain location in the downstream region [2] and is also reported by Sinha et al [9] whose experimental result on centerline effectiveness is shown in Fig.5 [9]

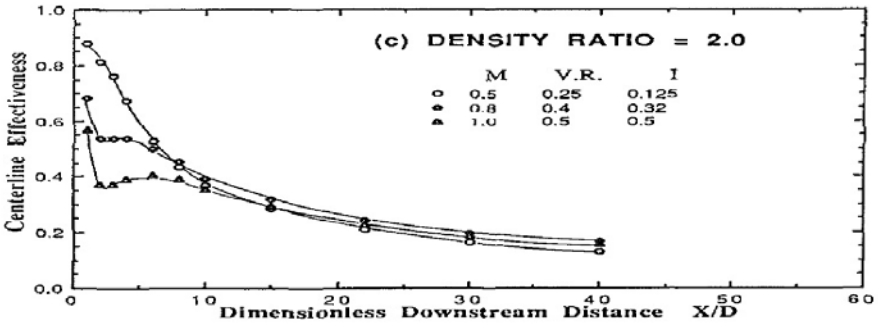


**Fig. 5 Centerline adiabatic effectiveness for various blowing ratios at density ratio of 2 [9]**

2. Density Ratio(D.R):

The coolant jet separation from surface was due to the high momentum of jet and the density ratio is related to the mass flux ratio [2] as in (2), the change in density ratio affects the performance of the coolant. Sinha et al [9] reported that the increase in density ratio results in a decrease of film cooling effectiveness as shown in Fig.6 [9]

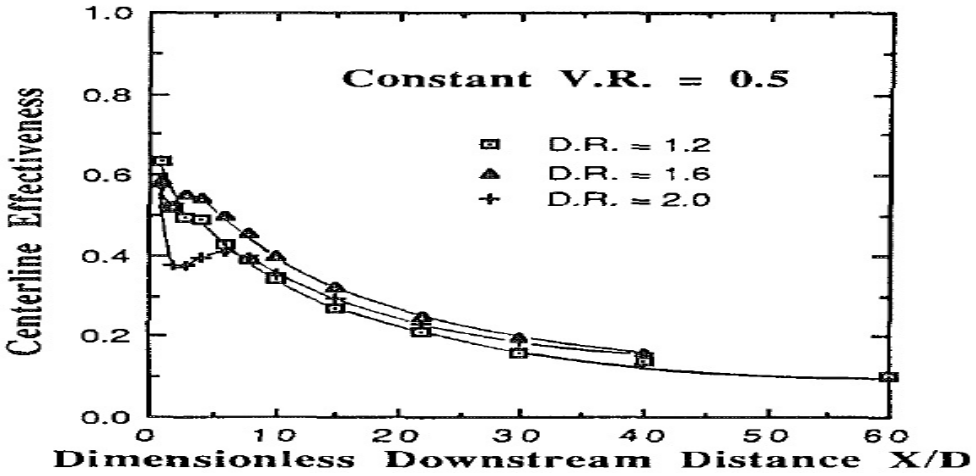


**Fig. 6 Centerline adiabatic effectiveness for various density ratios at velocity ratio of 0.5 [9]**

3. Hole Geometry:

The shape of coolant jet exit plays a significant role in film cooling effectiveness. In shaped hole the momentum of coolant jet was decreased and remained attached [2] which resulted in better effectiveness for shaped hole.

4. Injection angle:

The configuration of coolant hole injection results in a major change in performance of film cooling. The coolant injected at a certain angle to the mainstream flow is defined as the compound angled hole [2]. The compound angled hole is employed because the coolant exits from the hole turns towards the direction of the mainstream flow and provides better cooling performance.

5. Length of Hole:

The coolant exit velocity profile has a significant impact on the film cooling performance, which depends on the length of coolant hole. Thole et al [3] mentioned that detachment and reattachment of coolant jet occurred at the low L/D ratio and not for higher L/D ratio. Marc and Jubran [18] found that for L/D < 5 the variation of film cooling effectiveness was

negligible. Another detailed computational study from Azzi and Jubran [10] observed that film cooling effectiveness was increased for an increase in the L/D ratio.

### 1.3 Improved Cooling Techniques

In aircraft gas turbine engines the coolant is extracted from compressor as bleed air, which indirectly pays the penalty of decrease in performance of the Engine. Researchers over the decades focused on improving the cooling performance with the use of the minimal amount of coolant air extracted from compressor. The current approach is also an attempt to enhance film cooling performance through use of micro-holes, whereas a substantial amount of work on macro-hole film cooling has been done by researchers to improve the film cooling performance.

#### 1.3.1 Advancement in Film Cooling Technology

Researchers of modern gas turbine engines are focusing on increasing TIT, which indirectly demands improvement in the cooling performance of the engine. Recently, numerous efforts were made for increasing Film Cooling Performance,

- Azzi and Jubran [11] numerically proved that the converging slot-hole/console delivered better cooling performance than a cylindrical and shaped hole, where the console geometry resulted in good lateral spreading and minimise the effect of secondary vortices.
- The use of semi-circular holes by the Asghar and Hyder [12] resulted in performance similar to the circular hole, but the two staggered row of semi-circular holes, resulted in better effectiveness than the circular holes and the secondary vortices were weak and smaller in size than the vortices from the circular holes.
- The Experimental work from Sriram and Jagadeesh[13] installed micro jets for cooling on the stagnation region of the blunt body. They observed that the micro jets travelled long distance without mixing with the mainstream, resulted in better performance than macro-hole without any changes in aerodynamics behaviour of the flow.
- The Experimental work from Li et al [14] followed a novel idea in increasing the film cooling performance by varying the height of a micro slot and found that the micro-scale film performed better than the macro-scale film cooling.
- The recent experimental work from Hassan et al [21] found that the micro-tangential-jet (MTJ) provided superior performance than shaped coolant exit scheme. The application of

MTJ resulted in better lateral spreading of the coolant and penetrated longer distance without getting mixed.

An attempt for increasing the performance of film cooling was mainly focused on the experimental and computational works mentioned above and was found that decrease in coolant hole exit area increased the performance with minimum amount of coolant usage. The micro jet from the slot had deeper penetration into the mainstream flow without mixing which resulted in better cooling performance than the macro jet film [14]. The micro jets maintained its structure without breakdown and provided better cooling performance in immediate vicinity region of the coolant hole. Present work focused on analysis of film cooling performance through application of micro-hole with 200μm in diameter.

# Chapter 2: Numerical Approach

## 2.1 Introduction

The advancement in computer technology economically made life easier for researchers in film cooling. This chapter will discuss the computational techniques that were used for validating the predicted film cooling effectiveness results and flow structure as discussed in the previous chapter. The computational model was created in GAMBIT and was based on the experimental model of Sinha et al [9]. Moreover the discrepancies in results due to change in turbulence model will also be discussed in this chapter. Due to effective use of the available computational resources the two-equation k-ε turbulence model is the best turbulence model for this problem, which was used for comparison.

## 2.2 Notable computational studies

To perform a computational analysis on film cooling, it was necessary to gather knowledge from the previous relevant research. A significant number of computational studies have been available to understand the film cooling performance and coolant jet behaviour. Some of the relevant investigations will be discussed in this section.

Walters and Leylek [7.8] conducted a numerical investigation of film cooling and their results were compared with experimental work and were able to accurately capture the jet lift-off and reattachment at higher blowing ratios. A detailed study on the behaviour of seven different turbulence models on film cooling was reported by Ferguson et al [15] and it was concluded that the results from computational domain were mainly dependents on proper numerical modelling, quality of grids, use of higher order discretization scheme and also on the selection of turbulence model. Another study from Na et al [16] computationally analyzed the film cooling performance on a flat plate and found that the centerline effectiveness was predicted by a turbulence model and the laterally averaged effectiveness was predicted correctly by another turbulence model. Rajappan and Mahalakshmi [19] provided information about grid generation techniques and investigated the turbulence model behaviour at high mainstream turbulence intensity. Azzi and Jubran[10] numerically analyzed the film cooling performance for short length injection with multi-blocked grids and by the application of anisotropic turbulence model, whereas Azzi and Jubran[11] in another study numerically investigated performance of console geometry model with the application of DNS turbulence model. The latest study by Asghar et al [12] employed a

computational domain of semi-circular model and investigated the performance of film cooling through the application of realizable k-ε model.

The computational works mentioned here are some of the relevant detailed studies on film cooling performance. The study from Walters and Leylek [7, 8] used tetrahedral grids whereas the advancement on computer technology allowed the next generation researchers to use quadrilateral non-conformal grids and a higher order discretization scheme. Some researchers currently are using DNS/LES turbulence model which take significant computational resources. The common conclusion from the mentioned studies is that the solution of the computational domain was mainly dependent on high quality grids, use of higher order discretization scheme and selection of effective turbulence model. The use of DNS/LES turbulence model needed a lot of computational memory. Present analysis was carried out by the application of two-equation realizable k-ε turbulence model for effective use of the available computer resources. The grid generated and numerical setup for the present work has been discussed in the following sections.

## 2.3 Computational Model

### 2.3.1 Geometry

The simulated computational domain was modelled in GAMBIT shown in Fig.7. The geometry was selected from the experimental work of Sinha et al [9] and also it was similar to the computational model of Walters and Leylek [7, 8]. A condition of symmetry was assumed along the centerline of the coolant hole.

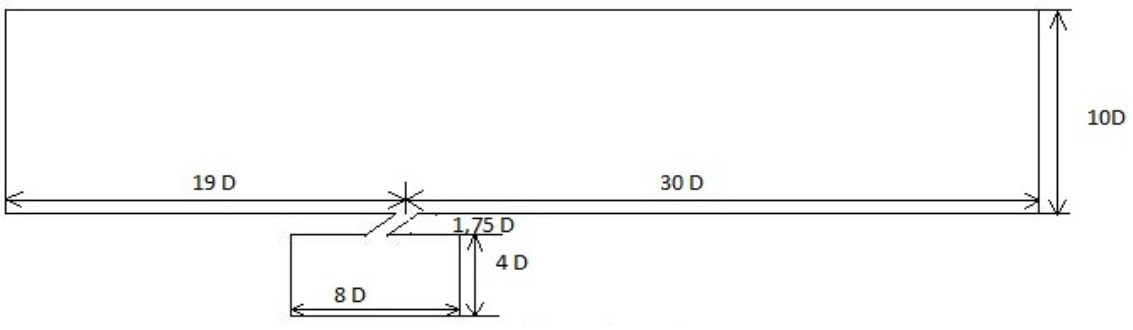


**Fig. 7 Model used for simulation**

The coolant hole of diameter 1.27cm located at a distance of 19D downstream from the leading edge of the plate, was extended to 30D downstream from the coolant hole, coolant from

the plenum of dimension 4D X 8D was made to enter into coolant hole of L/D ratio 1.75. Pitch between the holes was 3D and geometry was extended 10D above the hole. The coolant hole was inclined to a compound angle of $35^{o}$ to the mainstream flow.

### 2.3.2 Grid generation

The grid generation in numerical analysis was the key to get computational solutions. The complex flow structure of coolant at the hole exit region gave importance to grid generation in film cooling. The grid shown in Fig.6 modelled using GAMBIT was used to predict the complex flow structure in the vicinity region. The geometry was meshed with high quality grids without discontinuity and with minimal skewness. The near wall region was meshed with more care due to the turbulence nature of the flow.

Geometry was meshed with conformal, structured grids as shown in Fig.8 and was divided into three blocks mentioned by Azzi and Jubran [10]. In block-1 the coolant hole vicinity region was meshed with highly refined grids to capture the flow structure in the vicinity region and coarse grids in the downstream region to predict results with reasonable discretization error. The near wall region needs highly refined grids to capture the turbulence nature of the flow and to maintain the $y^{+} \leq 1$. Block-2 was meshed with highly refined grids in the region which connects block-1 and block-2 to capture the complex flow structure and to predict the turbulence behaviour of the coolant which exits through the hole. The region which connects block-2 and block-3 are meshed with highly refined grids to capture the low momentum region and jetting region as described by Walters and Leylek [7]. The minimum grid skewness is maintained for all three blocks.

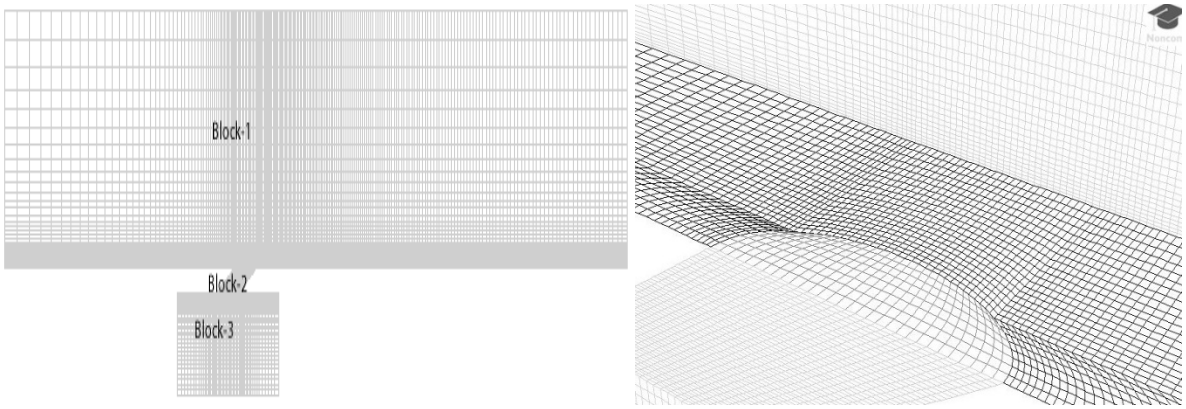


**Fig. 8 Sample grid for simulation**

## 2.4 Validation

FLUENT was used to study the jet in cross flow, to determine whether it was consistent in capturing the complex flow structure, so validation of generated computational grid was necessary. The flow structure from FLUENT was validated by comparing the computed film cooling effectiveness with the experimental results of Sinha et al [9]. For effective use of the available computational resources, grid independent test and turbulence behaviour of the cross flow was studied from the available turbulence models in FLUENT as discussed below

### 2.4.1 Governing Equations

The basic governing equations of fluid dynamics are conservation of mass, momentum and energy which speaks about physics of the problem is the cornerstone in Computational Fluid Dynamics. Vector form of the three equations is as follows

i) Conservation of mass

$$\frac{\partial \rho}{\partial t} + u_k \frac{\partial \rho}{\partial x_k} + \rho \frac{\partial u_k}{\partial x_k} = 0 \qquad (_0)$$

ii) Conservation of momentum

$$\rho \frac{\partial u_j}{\partial t} + \rho u_k \frac{\partial u_j}{\partial x_k} = \frac{\partial \sigma_{ij}}{\partial x_j} + \rho f_j \qquad (_0)$$

iii) Conservation of energy

$$\rho \frac{\partial e}{\partial t} + \rho u_k \frac{\partial e}{\partial x_k} = \sigma_{ij} \frac{\partial u_j}{\partial x_i} - \frac{\partial q_j}{\partial x_j} \qquad (_0)$$

equations 2-4 are basic vector form of governing equations. The flow of coolant involves the viscous behaviour, so the Navier-Stokes equation was employed to solve the problem. CFD researchers on film cooling have concluded with various suggestion of turbulence model to solve the film cooling problem due to the turbulent nature of the flow. Numerous turbulence models are available in FLUENT but there is no specific turbulence model specified to capture the complex behaviour of film cooling. Therefore turbulence-viscosity model was validated with experimental results and proceed with further changes to achieve better results with minimum error.

### 2.4.2 Turbulence Model

Previous CFD studies in film cooling suggest different turbulence model to capture the complex flow structure of film cooling. A detailed turbulence model analysis for film cooling from Ferguson et al [15] concluded with the two layer standard k-ε model predicts the results better than the RNG and RSM turbulence model and also mentioned that the two-layer near wall treatment was not suited in plenum region due to low Reynolds number. The detailed computational study by Walters et al [7, 8] found that the two-layer standard k-ε model behaves better than the other models. Standard k-ε model with changes proposed by Bergeles was used by Azzi and Jubran[10] whereas another study from Azzi and Jubran[11] found that k-ε model was not suitable for modelling the complex cross flow structure and used DNS based two-layer model. The computational work from Na et al [16] proved that for flat plate, the centerline effectiveness was well predicted by realizable k-ε model and laterally averaged effectiveness was predicted by the S-A model. Asghar et al [12] used two-layer realizable k-ε model to predict the flow structure from semi-circular holes. Ely and Jubran [17] used realizable k-ε model to predict the effect due to the use of sister hole. However other turbulence model such as LES, DNS have higher potential to capture the complex flow structure but they are computationally expensive and need more memory and time to run the simulation. So the current work will made comparison between the "two equation" standard k-ε and realizable k-ε turbulence model with two-layer near wall treatment and better one is used for further analysis.

### 2.4.3 Numerical Setup

The grid generated in GAMBIT, was solved with FLUENT 14 available in the High Performance Computing Virtual Laboratory (HPCVL) from Queens University. The steady-state, three-dimensional double precision (3DDP), pressure based Navier-stokes equation was used to predict the film cooling flow field. Air was selected as a continuum which obeys incompressible-ideal gas law and plate is considered to be made up of Aluminium with standard properties assumed in FLUENT, operating pressure was set as 101235 Pa and Gauge pressure as 0 Pa. The boundary condition was set based on the experimental work of Sinha et al [9] as shown below in Table.2. Higher order schemes were employed to solve the equation for better accuracy in solution and pressure-velocity coupling equation was solved through the use of SIMPLE algorithm. The simulation was run in 12 processors and continuously for 8hrs.

**Table 2 Boundary conditions for simulation**

| Property | Value |
|---|---|
| Mainstream Velocity | 20m/s |
| Mainstream Temperature | 300 K |
| Blowing Ratio | 0.5 |
| Density Ratio | 2 |
| Coolant Temperature | 150 K |

The turbulent length scale for the mainstream flow was calculated as $L_t$=0.05h and for the coolant as $L_t$=0.07$D_h$, where h is the height of the domain from the plate and $D_h$ is the hydraulic diameter of the coolant inlet section. The turbulent boundary conditions used for the present simulation given in the Table.3 is based on the information available in the Fluent Inc.

**Table 3 Turbulence boundary conditions for simulation**

| Continuum | Turbulence Intensity (%) | Turbulent Length scale(mm) |
|---|---|---|
| Mainstream | 1 | 6.35 |
| Coolant | 1 | 0.889 |

### 2.4.4 Grid Independent Study

FLUENT generates the results depending upon the input condition in Table.2 and Table.3 but the accuracy and stability in the solution depends on the grid generated in GAMBIT. The number of nodes for each grid was increased by increasing the number of nodes at the edge of geometry by 10% from the initial grid, computed film cooling effectiveness was compared for all generated grids and selected grids depend on stability in the solution. There are nearly six to seven grids generated and the results of the initial and final two grids were compared as shown in Fig.9, where the variation in the effectiveness calculated from Mesh-1 and Mesh-2 was found to be larger than the variation between Mesh-2 and Mesh-3. For effective use of available computational resources the Mesh-2 with 2.3 E+5 nodes was selected to carry out the validation of the experimental results.

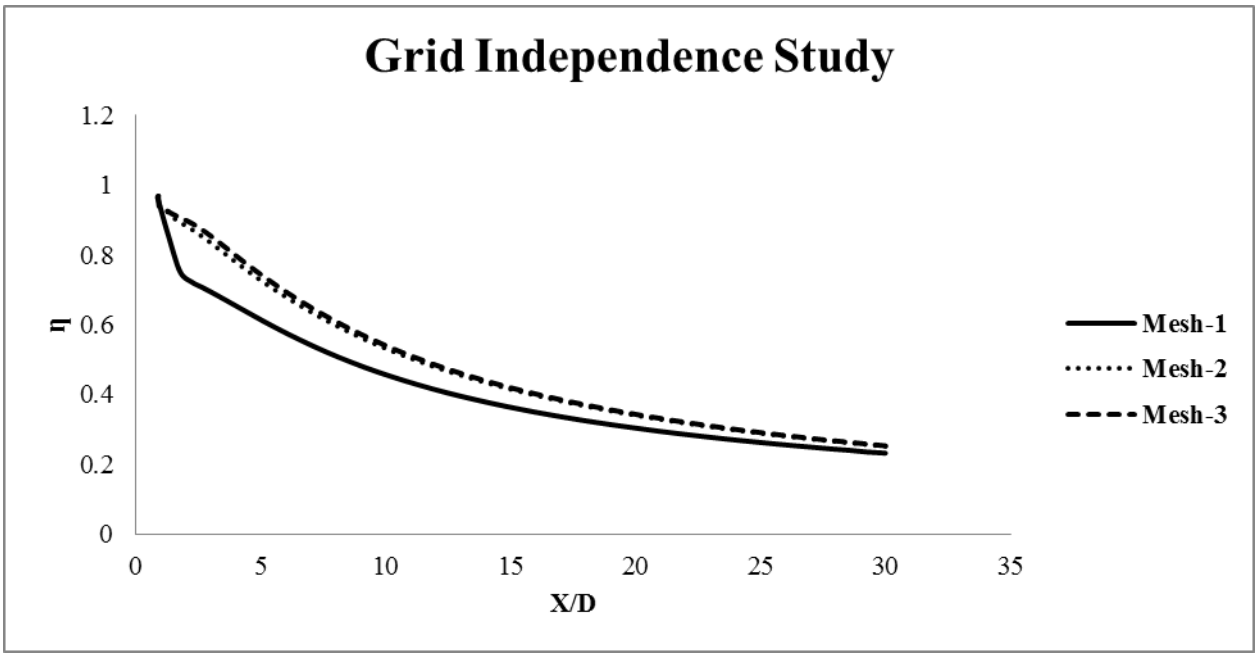


**Fig. 9 Grid independence study**

### 2.4.5 Turbulence Study

The comparison was made between the behaviour of the standard and realizable k-ε turbulence models with two-layer near wall treatment and is discussed in this section. Fig.10 shows the comparison of the centerline adiabatic effectiveness between two turbulence model at low blowing ratio (M=0.5) with experimental result of Sinha et al [9]. The standard k-ε (SKE) and realizable k-ε (RKE) turbulence models predict close to the experimental results in the vicinity region of x/D < 5 and deviate in the downstream region. The discretization error for the RKE model is less than the SKE model in the region of 5<x/D<20 and in remaining region both the models show very little variation from each other.

Fig.11 compares the centerline adiabatic effectiveness of two turbulence models at high blowing ratio (M=1) with the experimental result of Sinha et al [9]. The results of both SKE and RKE models over predict the experimental result. In downstream region of x/D > 4 the RKE model predicts the result close to the experimental result than the SKE model.

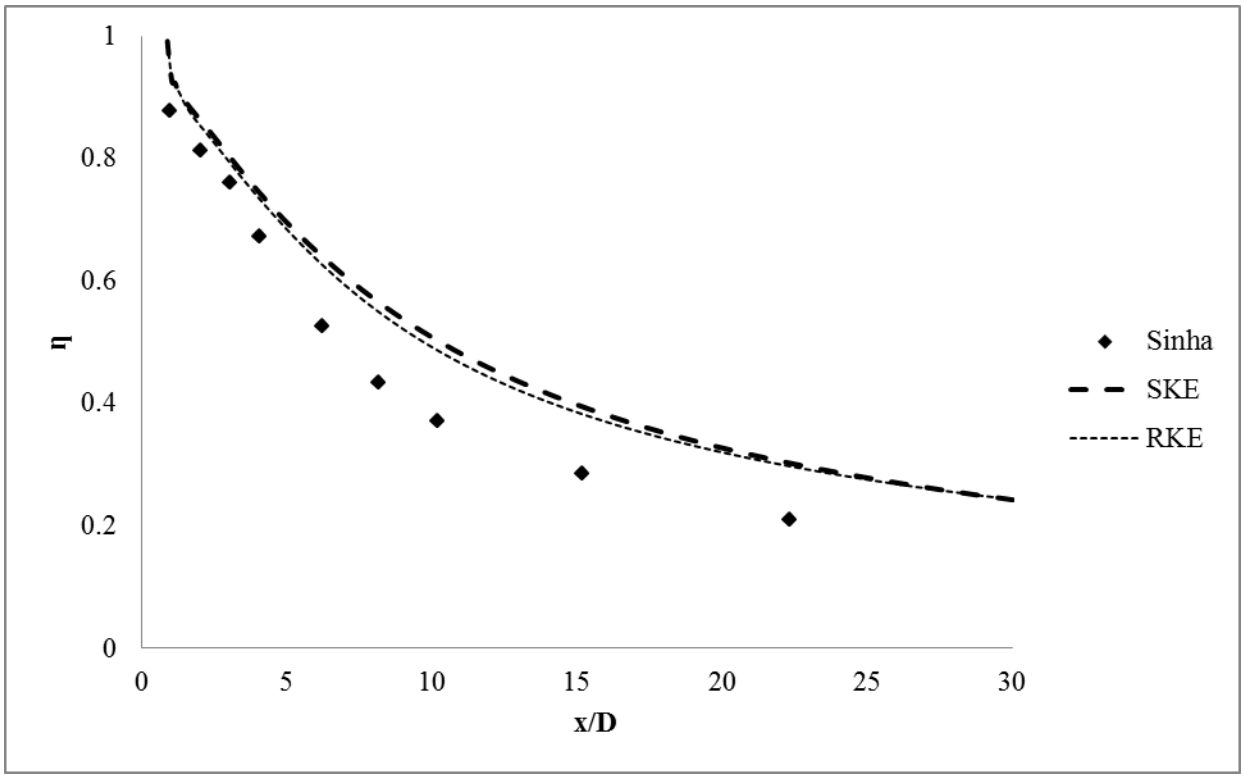


**Fig. 10 Centerline effectiveness at low M (M=0.5)**

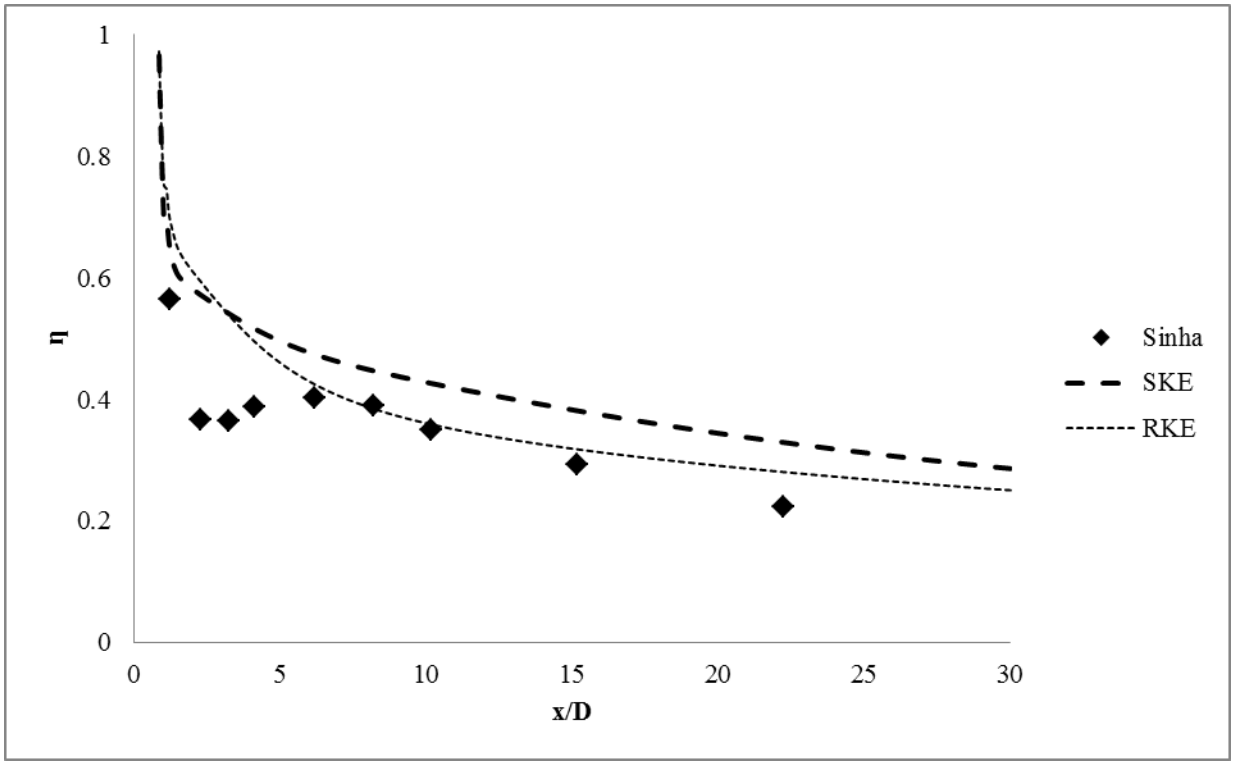


**Fig. 11 Centerline effectiveness at high M (M=1)**

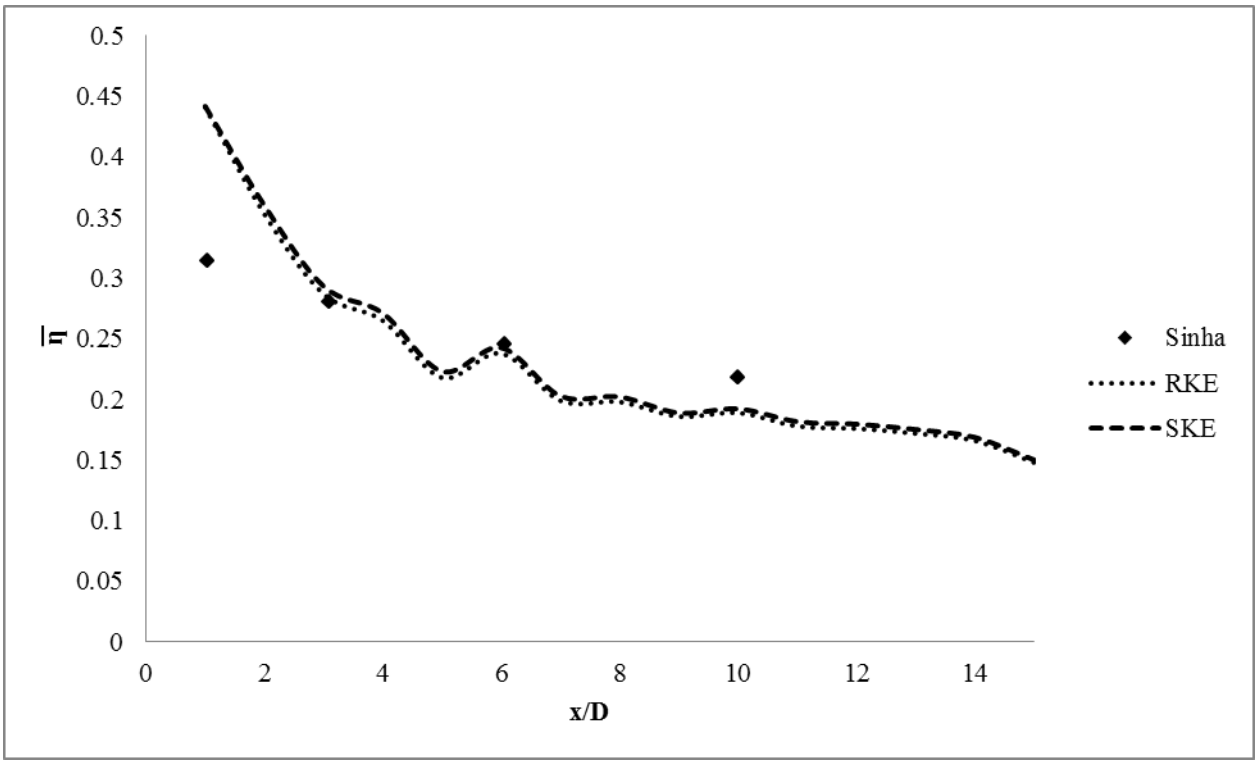


**Fig. 12 Laterally averaged effectiveness at low M (M=0.5)**

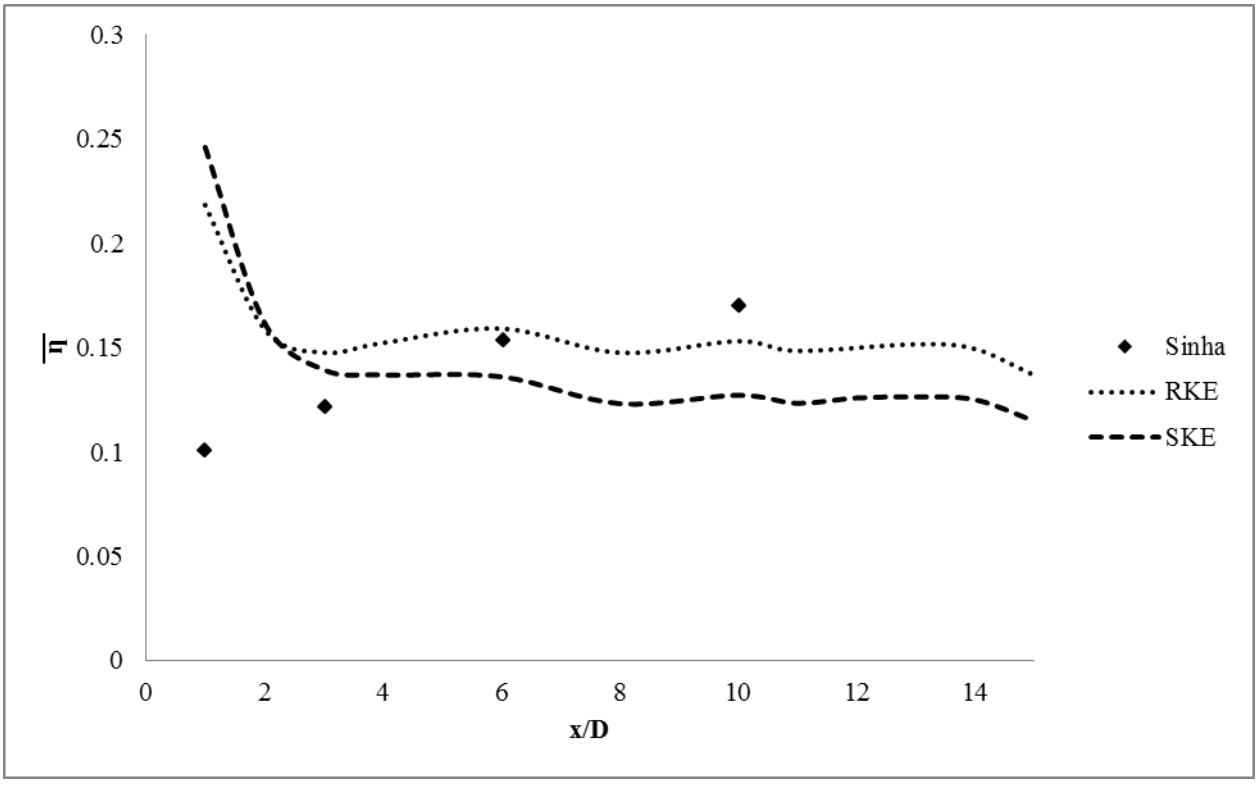


**Fig. 13 Laterally averaged effectiveness at high M (M=1)**

Fig.12 and Fig.13 show the comparison of turbulence models for laterally averaged effectiveness at both blowing ratios. Both the models over predict the experimental result in vicinity region of $x/D < 4$ while in region of $x/D > 4$ both turbulence models under predict the experimental result. At low blowing ratio, the turbulence models show little variation from each other. However at high blowing ratio in vicinity region of $x/D < 4$ both models over predict the experimental results, whereas in the downstream region of $x/D > 4$ the deviation between the experimental result and the computed result of the RKE model is less than the SKE model.

In conclusion, it is evident from the above discussion that the RKE model predicts better than the SKE model, thus the RKE model is used for further analysis of the micro-hole film cooling.

# Chapter 3: Micro-hole Analysis

## 3.1 Introduction

The application of micro-holes in film cooling research is a novel approach on increasing the cooling performance by using a minimum amount of coolant. Significant number of work were available on “macro-holes” however only a few works were available on micro scale film cooling as mentioned in section 1.3.1. The work from Azzi and Jubran[11] promises a better cooling performance by reducing the coolant exit area. Asghar and Hyder[12] determined that the semi-circular hole achieves same effectiveness and the application of two staggered semi-circular holes achieve better effectiveness than the fully circular macro-hole. Sriram and Jagadeesh [13] experimentally studied the application of micro-jet in the front face of blunt body results in better effectiveness and the jet travels long distance without getting mixed with the mainstream air. An another experimental work from Li et al[14] on micro slot cooling determines that the flow from micro slot travels longer distance than macro slot jet without break and achieve better effectiveness by the use of a minimum amount of coolant. The above investigations report that the improvement in film cooling performance was due to reduction in the coolant exit area. The advantage on the application of micro-holes in film cooling is to reduce the amount of coolant used.

However the application of micro-hole in film cooling process has a major disadvantage of “blockage” in the coolant hole due to the debris from mainstream and coolant air. During take-off and landing aircraft gas turbine engine can be subjected to the conditions of debris entered through the inlet of the engine. The particulates which pass the combustion chamber get heated and become molten. When molten particulates hit the coolant holes they could stick and become partially solidified, which is a common problem in aircraft gas turbine engines. Since the current work focuses on detailed computational analysis on the performance of micro-hole film cooling, the analysis of coolant hole blockage will be recommended for future work.

This chapter will discuss about the computational model for micro-hole film cooling analysis. The boundary conditions and operating parameters used in this study are the same as those used for validation in chapter 2.

### 3.2 Micro-hole Model

#### 3.2.1 Computational Domain

Limited number of studies on micro-jet film cooling analysis made it difficult to model the computational domain for further analysis. The computational domain plays a major role in capturing the complex flow structure. From the study of Azzi and Jubran [11] it was found that modelling converging slot model was based on dimensionless parameters used for the computational domain of the experimental model from Sinha et al [9], but the present work focus on the computational analysis of the application micro-hole of 200μm diameter on the same experimental model. The dimensionless parameters for upstream and downstream region from the hole, the parameters used for plenum and the top extend region from the plate are kept the same as shown in Fig.7. The L/D ratio of computational domain shown in Fig.7 depends on the thickness of plate used by Sinha et al [9], so the use of same L/D ratio for micro scale model was not a good practice of comparison. The application of micro-hole on the experimental model of same thickness leads to L/D ratio of 111.13. The result from Azzi and Jubran [10] shows that for L/D >5 in macro-hole, a negligible increase in effectiveness was mentioned which was also mentioned by Ely and Jubran [17]. Due to an insufficient amount of work in micro jet analysis and for efficient use of available computational resources, the behaviour of flow in the micro jet pipe was studied first for various L/D ratios and the result of the optimal L/D ratio was compared with the results of a macro-hole model.

A multi-block conformal, structural grid was generated as mentioned before in section 2.3.2. The grid independence study has been performed and the optimal grid of 2.5E5 nodes was selected to carry out the analysis of micro-hole model. In order to solve the viscous sub-layer region, grids near the plate is adjusted to maintain the $y^{+} \leq 1$.

#### 3.2.2 Numerical Setup

The micro-hole computational domain was solved using FLUENT 14. The working condition was same as that of macro-hole model described in 2.3.3. Realizable k-ε turbulence model was used to predict the flow field for the micro-hole model. The boundary conditions used were same as mentioned in Table.2 and the turbulence parameters are determined as mentioned in section 2.3.3. The turbulence parameter for the micro-hole model was shown in Table.4.

**Table 4 Turbulence parameters for micro-hole**

| Continuum | Turbulence Intensity (%) | Turbulent Length scale(mm) |
|---|---|---|
| Mainstream | 1 | 0.1 |
| Coolant | 1 | 0.014 |

### 3.3 Micro Flow Behaviour

The behaviour of micro flow in film cooling has been mentioned by some of the studies mentioned previously in section 1.3.1. The experimental study of Li et al [14] found that the performance of micro film cooling was based on height of the slot. The use of smaller slot height results in better performance and smaller amount of coolant is used than the larger slot. Another experimental work from Sriram and Jagadeesh [13] observed that the array of micro jets results in better performance than the single jet and injection of coolant from the micro jets with low momentum did not provide significant changes in aerodynamic forces. The recent experimental work from Hassan et al [21] showed that the MTJ scheme performed much better than the shaped exit scheme model and they observed that the decay of effectiveness on the suction side was less than the pressure side of the turbine vane. The common conclusion from the micro film cooling is that the flow penetrates a long distance and use less amount of coolant. The studies mentioned have discussed the performance of the micro jet cooling which provides better performance at high blowing ratio due to the large amount of coolant used for cooling. The disadvantage is the increase in pressure drop at high blowing ratio and thermal stress at the lip of the micro slot was also observed by Hassan et al [21].

The knowledge about the performance of jet from the micro slot has been studied from the works mentioned above. However physics in the behaviour of jet in micro-hole film cooling still needs further investigation. Current work predicts the behaviour of jet in the micro-hole for the various L/D ratio of coolant pipe.

#### 3.3.1 Film Cooling Effectiveness

The centerline adiabatic effectiveness of the micro-hole model for various L/D ratios at M=0.5 and M=1 are shown in Fig.14 and Fig.15. The centerline effectiveness is found to be lower for L/D ratio of 1.75 and reached the maximum at L/D ratio of 3.5, for L/D ratio greater than 3.5 the effectiveness starts decreased as observed in Fig.14. For all L/D ratio at low blowing

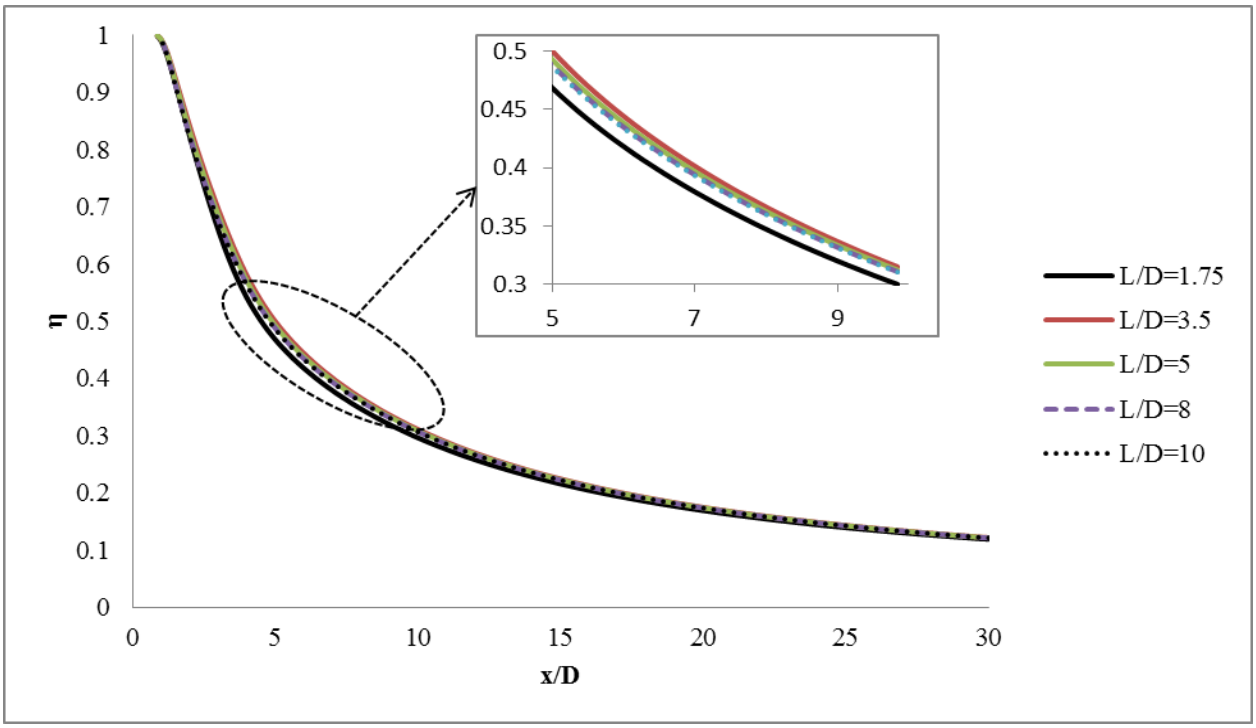


**Fig. 14 The Centerline adiabatic effectiveness of micro-hole for various L/D at M=0.5**

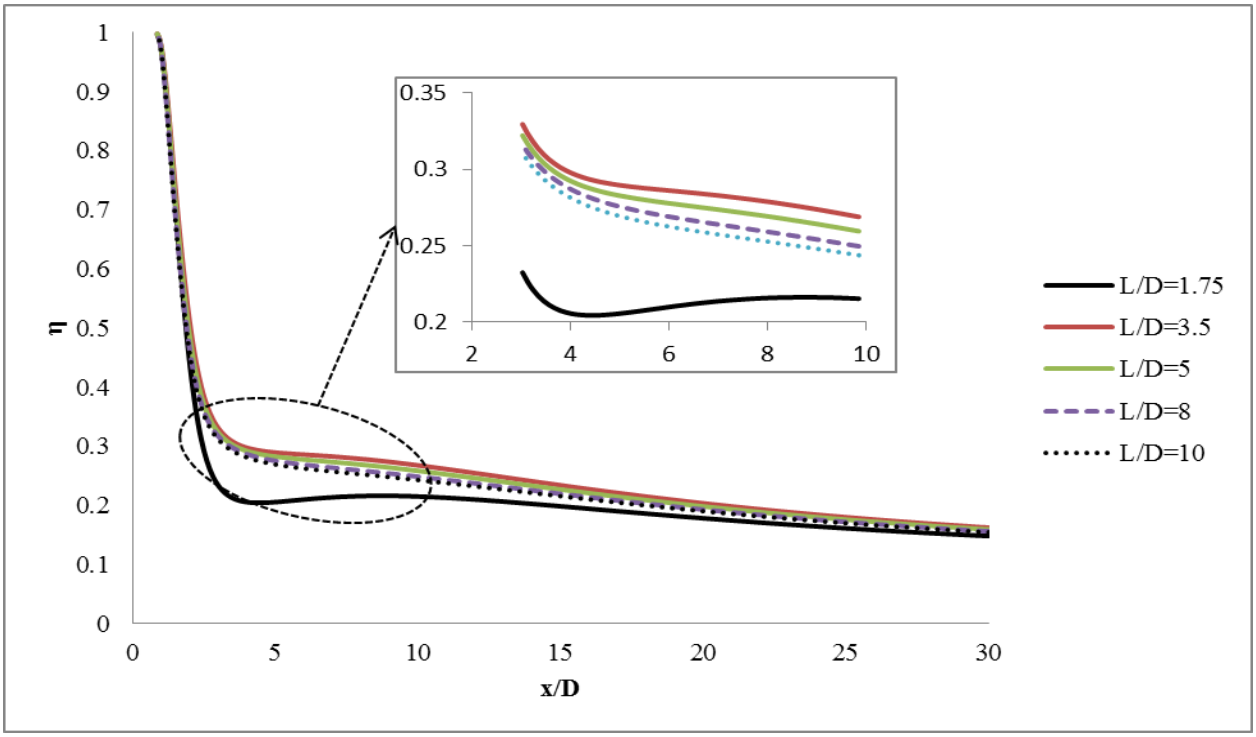


**Fig. 15 Centerline adiabatic effectiveness of micro-hole for various L/D at M=1**

ratio, the rate of decay in effectiveness is high in the immediate vicinity region of x/D < 4, for 4 < x/D< 20 the rate of decay in effectiveness is low and for the region of x/D > 20 the effectiveness stays close to stable. Moreover at high blowing ratio the effectiveness decays tremendously in the region of x/D < 3 at higher rate than at low blowing ratio for all L/D ratios due to jet lift-off from the surface. At high blowing ratio, the low L/D ratio in region of 3 < x/D < 10, the rate of decay in effectiveness changes drastically whereas at high L/D ratio the effectiveness decreases gradually in the region of x/D > 3. At high blowing ratio the jet lift-off occurred for low L/D ratio and the jet reattachment was disappeared as L/D ratio increases is shown in Fig.15.

The laterally averaged effectiveness for various L/D ratios and for two different blowing ratios is shown in Fig.16 and Fig.17.

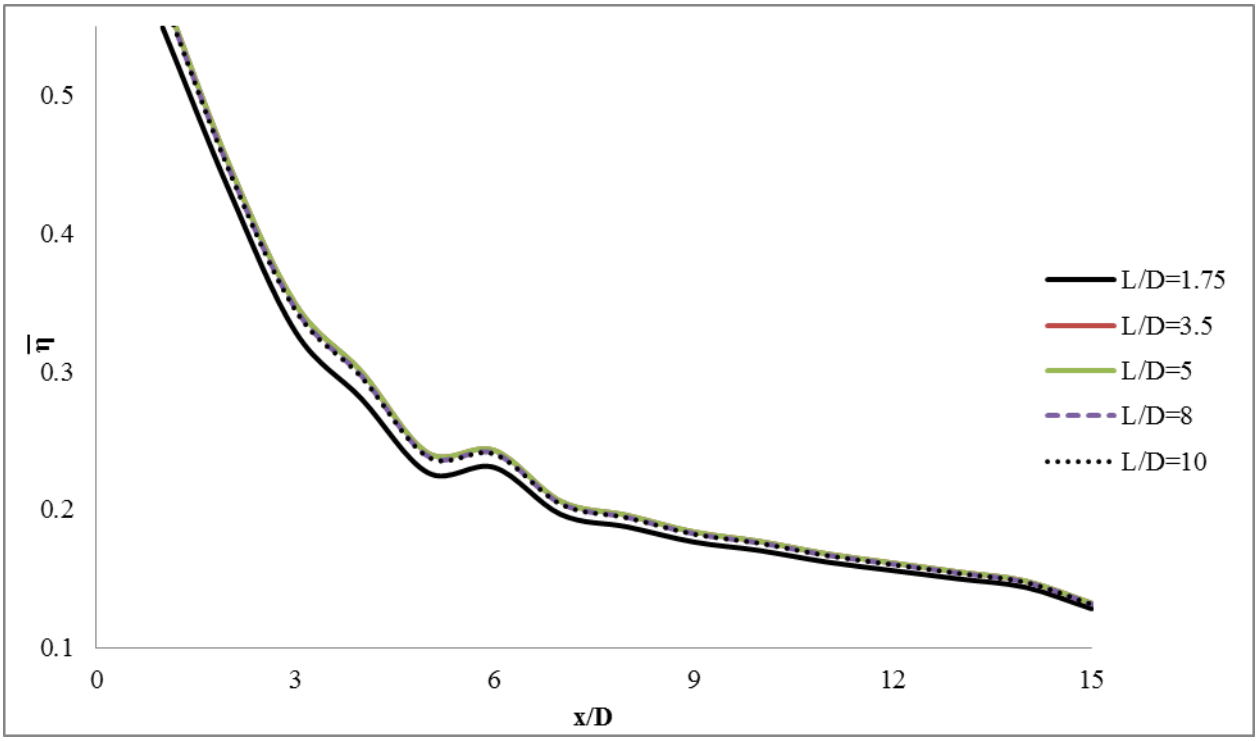


**Fig. 16 Laterally averaged effectiveness for micro-hole for various L/D at M=0.5**

The lateral distribution of coolant from the hole was extreme for L/D of 3.5 and lower for L/D ratio of 1.75, a further increase in L/D ratio behaves in a similar manner as centerline adiabatic effectiveness. For L/D ratio greater than 3.5 a slight variation in performance is observed at low blowing ratio whereas at high blowing ratio the variation between L/D ratio of 5

and 8 is found to be greater than the variation between L/D ratios of 8 and 10 which is similar to the centerline adiabatic effectiveness.

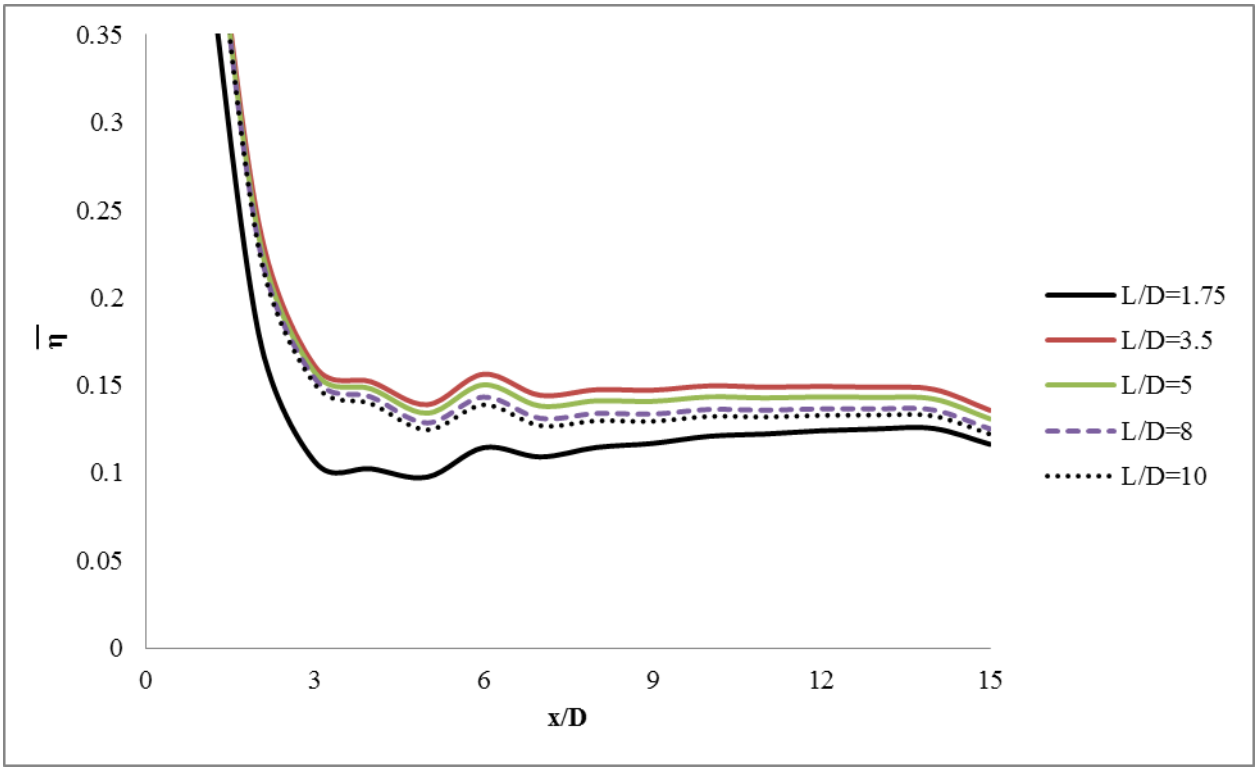


**Fig. 17 Laterally averaged effectiveness of micro-hole for various L/D at M=1**

The lateral distribution of coolant from the hole is found to be extreme for L/D of 3.5 and lower for L/D ratio of 1.75, a further increase in L/D ratio behaves in a similar manner as centerline adiabatic effectiveness. For L/D ratio greater than 3.5, a slight variation in performance is observed at low blowing ratio whereas at high blowing ratio the variation between L/D ratio of 5 and 8 is found to be greater than the variation between L/D ratios of 8 and 10 which is similar to the centerline adiabatic effectiveness.

The performance of the micro-hole film cooling for various L/D ratios is different from the macro-hole film cooling. The increase in L/D ratio results increase in the performance for macro-hole film cooling, where increase in the L/D ratio for micro-hole film cooling shows increase in performance till L/D of 3.5 and a further increase in L/D ratio results in a decrease in the performance.

### 3.3.2 Flow at Jet Exit

The injection of the coolant jet into mainstream flow results in a complex flow structure as mentioned in section 1.2.1, a considerable amount of experimental and computational studies have been conducted about the flow structure for macro-hole film cooling. From the analysis of micro-hole film cooling discussed in section 3.3.1, the unfamiliar physics of micro flow structure needs a detailed study of the jet in the coolant pipe. The velocity vectors of the coolant jet from the micro-hole for various L/D ratios at M=0.5 is shown in Fig. 18 and at M=1 in Fig.19

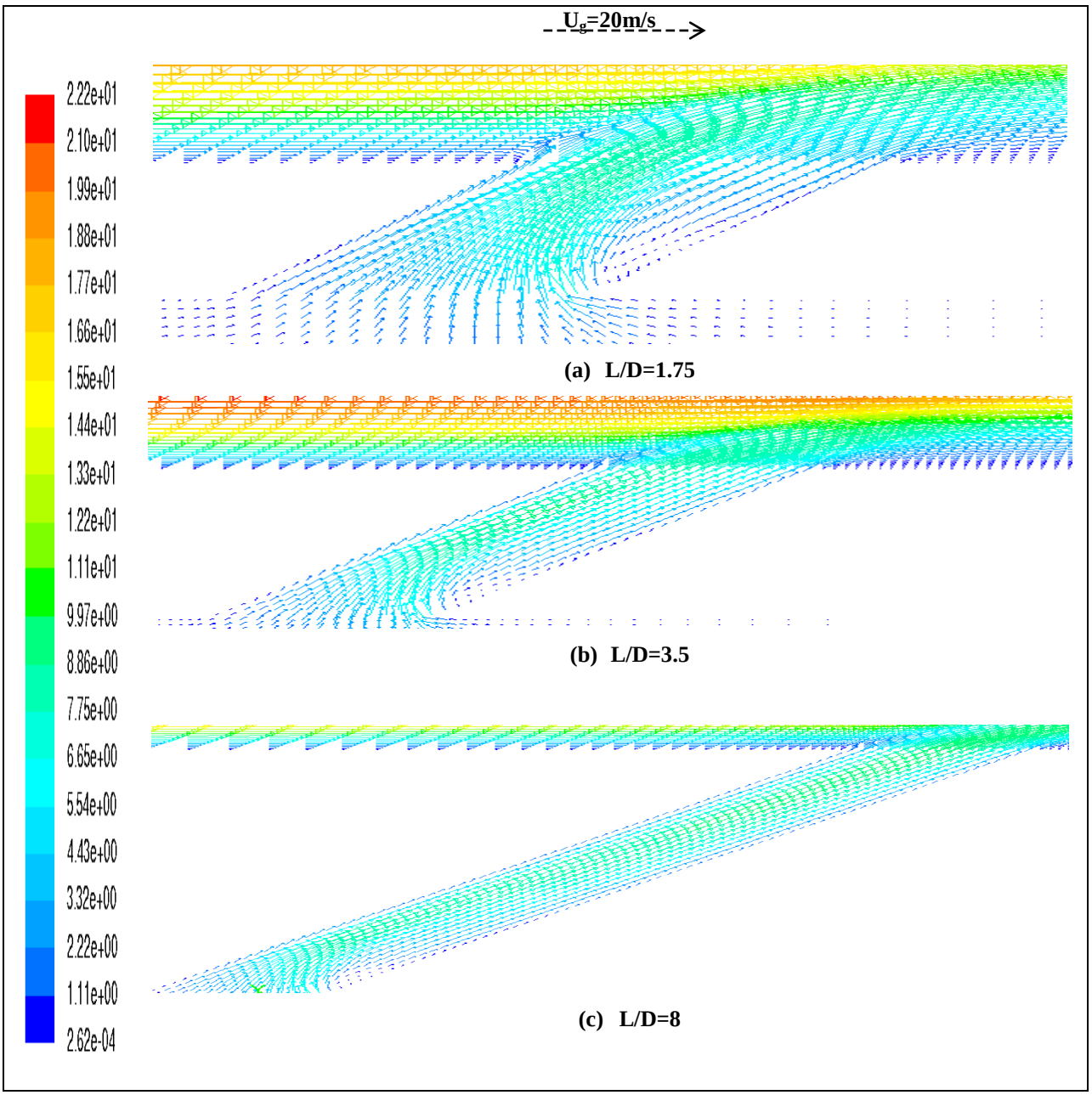


**Fig. 18 Velocity vectors along the centerline of the injection at M=0.5 for (a) L/D=1.75, (b) L/D=3.5 and (c) L/D=8**

Velocity profile at the exit of the coolant hole has a greater impact on the film cooling performance in the downstream region of the coolant hole [3]. The coolant enters into the hole from the plenum and gets separated on the trailing edge forms a low momentum region and gets accelerated towards the leading edge forms a coolant jetting region inside the hole as shown in Fig.18 and Fig.19

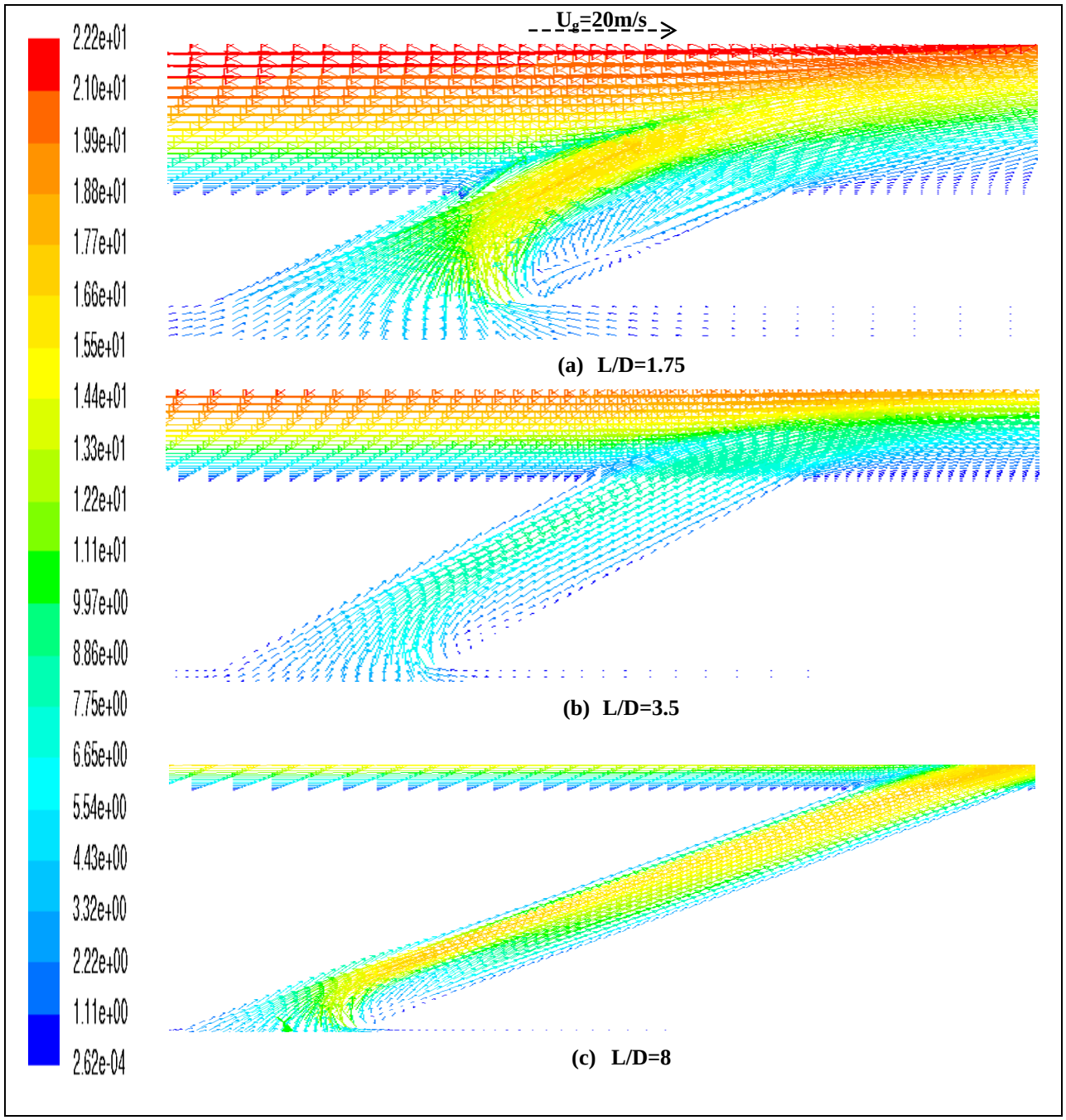


**Fig. 19 Velocity vectors along the centerline of injection hole at M=1 for (a) L/D =1.75, (b) L/D=3.5 and (c) L/D=8**

For shorter length hole of L/D ratio 1.75, the coolant exits before it gets reattached and results in highly skewed velocity profile on the leading edge as shown in Fig.18 and Fig.19. The velocity profile at the exit for M=1 is highly skewed than the M=0.5 due to the increase in momentum. Moreover, amount of coolant discharged from leading edge of the hole is greater than the trailing edge results low performance at L/D=1.75 for both blowing ratios.

For greater length holes with L/D ratios of 3.5 and 8 shown in figures, the coolant found enough time to reattachment in the coolant hole. For L/D ratio of 3.5, the coolant exits the hole before the flow becomes fully developed. The momentum of the coolant on the trailing edge of the coolant-hole is larger for L/D ratio of 3.5 than 1.75, results in large amount of coolant discharge from the trailing edge. The increase in amount of coolant discharge at the trailing edge of the coolant hole is responsible for maximum performance at L/D ratio of 3.5. For L/D ratio of 8, the flow becomes fully developed resulting in the velocity getting skewed at the centre region of hole and the amount of coolant discharged from trailing edge of the hole is less than the L/D ratio of 3.5. From the discussion it is clear that film cooling performance depends on the velocity profile at the exit of coolant hole.

The coolant performance for various L/D ratios is discussed through the plots and figures shown above. Indeed, the centerline adiabatic effectiveness shows a slight variation for L/D > 5. However, the variation on the laterally averaged effectiveness at high blowing ratio is greater for L/D ratios between 5 and 8 than the variation between 8 and 10. It is obvious from the plots that the flow from the hole with L/D of 5 shows jet lift off which is not observed in longer holes, so for the micro-hole model with L/D ratio of 8 is selected for comparison.

# Chapter 4: Comparative Study

## 4.1 Introduction

The comprehensive review in the performance of coolant jet from macro-hole and the computational analysis on performance from the micro-hole has been shown in the previous chapters. As mentioned before in section 3.2.1 the thickness of the experimental model plays a significant role in the comparative study. The L/D ratio of 1.75 for macro-hole model is not the same as that for the micro-hole. Application of micro-hole on the experimental model of the same thickness results in the L/D ratio to 111.13 which needs more computational memory, for effective use of available computational resources detailed study of coolant flow inside the coolant hole was made in the previous chapter. From the analysis of the micro-hole model from the previous chapter, it was found that the flow in coolant hole becomes fully developed for L/D ratio of 8. However for effective use of available computer resources, the computational model with L/D ratio of 8 has been chosen for the comparative study. The comparison between the performances of the macro-hole (experimental) model with L/D of 1.75and micro-hole model with L/D of 8 is carried out in this chapter. The effect due to the change in coolant exit diameter has been analyzed and discussed below.

## 4.2 Film cooling Performance

It is evident that at low blowing ratio the coolant jet remains attached to the surface. The study from Kohli et al[3] reported that for cylindrical holes the coolant jet starts lift-off from the surface at blowing ratio of M=0.5 and reattached in the downstream region, however the jet reattachment did not occurred for larger L/D ratio. Moreover the flow behaviour from the micro-hole is still unknown and need further investigation. The results from the macro-hole and micro-hole analysis at various blowing ratios were compared in the following section

### 4.2.1 Low Blowing Ratio (M=0.5)

Temperature contours is the best way to illustrate the effect of coolant on the hot plate. The temperature distribution at blowing ratio of M=0.5 from the macro-hole and micro-hole is shown in Fig. 20,

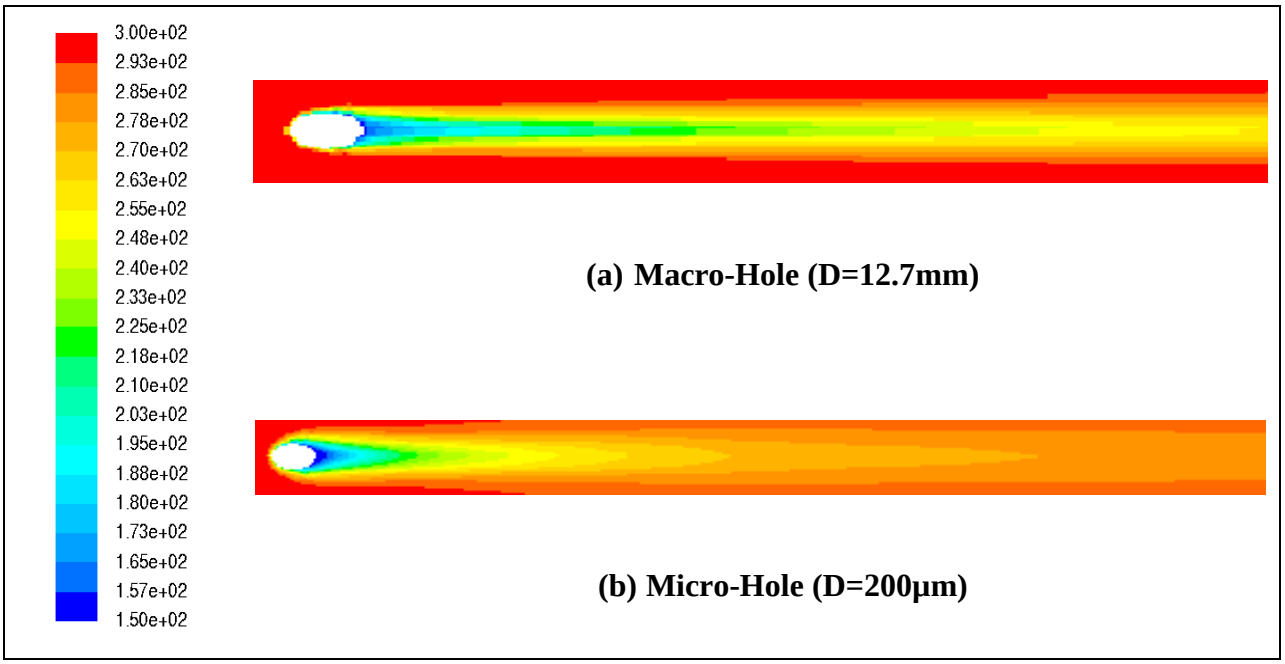


**Fig. 20 Temperature contour at M=0.5 for (a) macro-hole and (b) micro-hole**

The effect in the use of micro-hole on film cooling results in better distribution of the coolant in lateral direction than that for the coolant distribution from macro-hole. The temperature distribution on the hot plate is numerically documented as effectiveness of the film cooling.

The centerline adiabatic effectiveness in Fig.21 shows that the micro-hole performs well in the vicinity region of x/D < 1.7 and the effectiveness from the micro-holes decays faster in the downstream direction due to the jet lift off. For macro-hole, coolant jet lift-off shown in Fig.21 is due to greater momentum of the jet with respect to the mainstream mass flow [22]. Due to reduction in the coolant exit area, the amount of coolant from the hole exit is reduced, so the momentum of the coolant jet from the micro-hole is decreased. The decrease in jet momentum with respect to the mainstream flow provides better performance in the vicinity region. Fig.20 shows that the coolant distributes well in the lateral direction for coolant from micro-hole than the macro-hole, where the lateral coolant distribution is numerically recorded through the laterally averaged effectiveness as shown in Fig.22. Laterally averaged effectiveness from micro-hole and macro-hole was compared in Fig.21. The coolant from micro-hole performs superior than macro-hole for x/D > 7. The laterally averaged effectiveness did not provides detailed information about lateral distribution of coolant in the plate which was also agreed by Azzi and Jubran [11], for detailed information about the lateral coolant distribution of coolant the local

lateral distribution of effectiveness for the various location of x/D at (1, 1.7, 3 and 15) is shown in Fig. 23

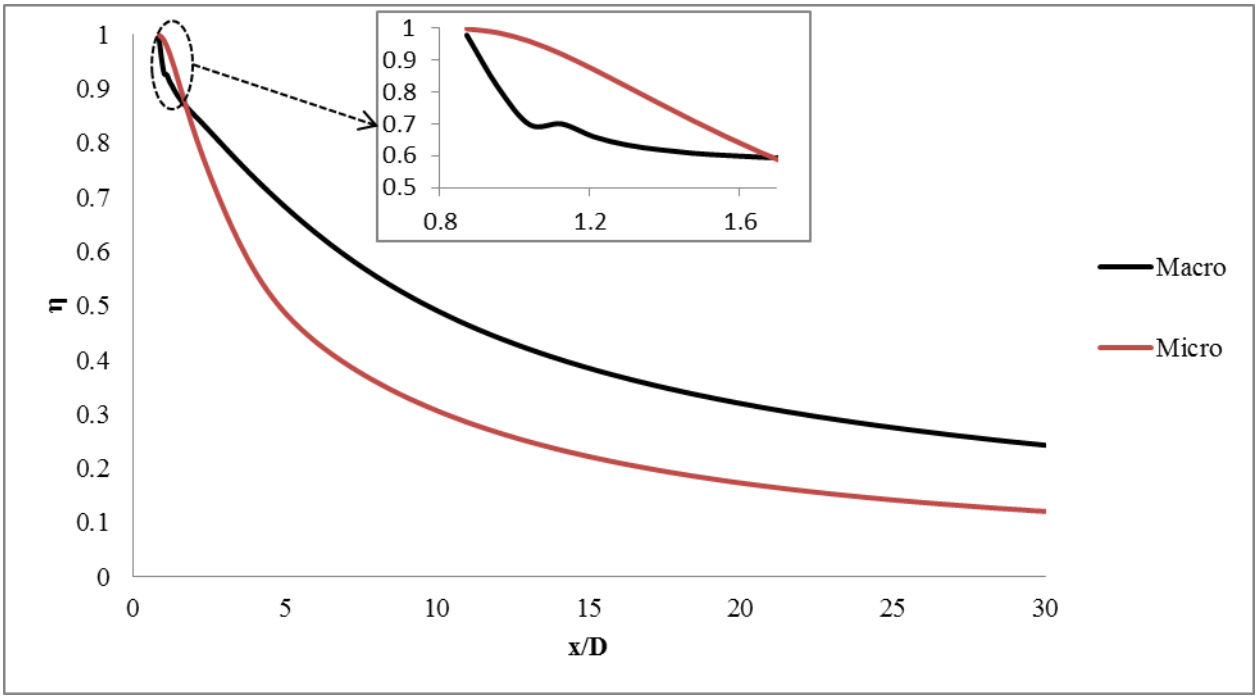


**Fig. 21 Comparison of centerline adiabatic effectiveness at M=0.5**

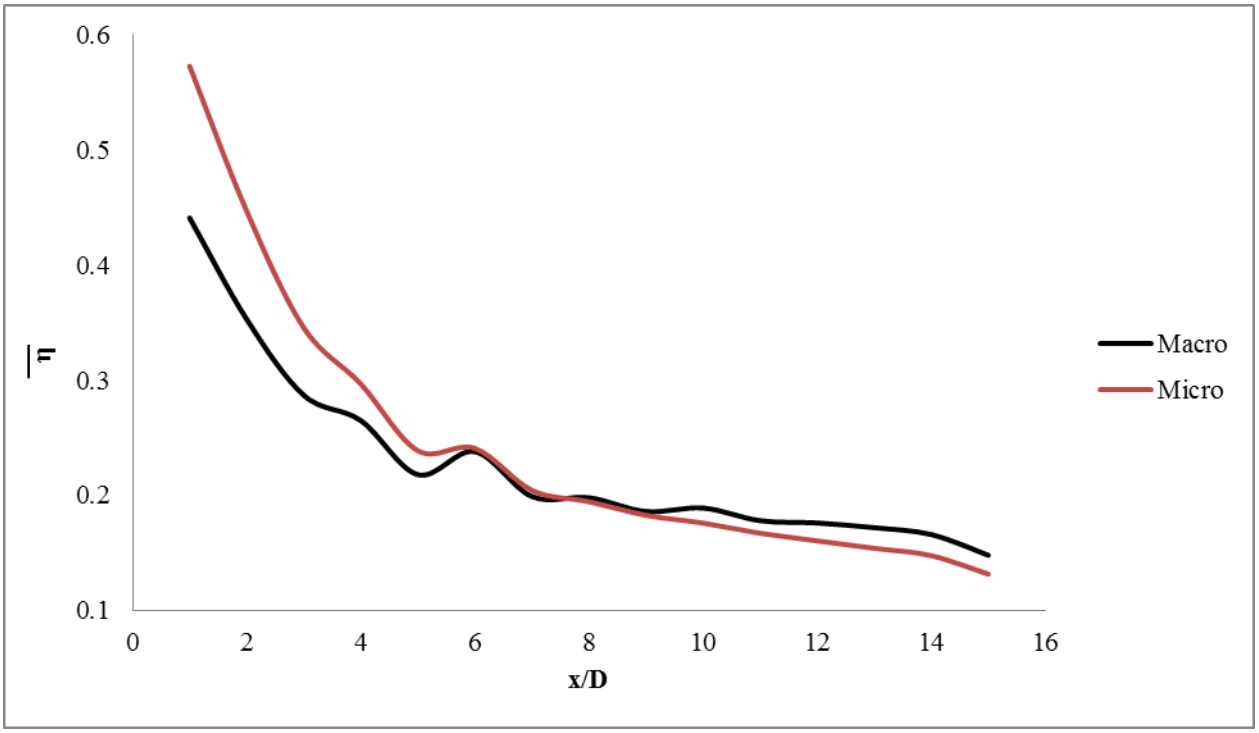


**Fig. 22 Comparison of laterally averaged effectiveness at M=0.5**

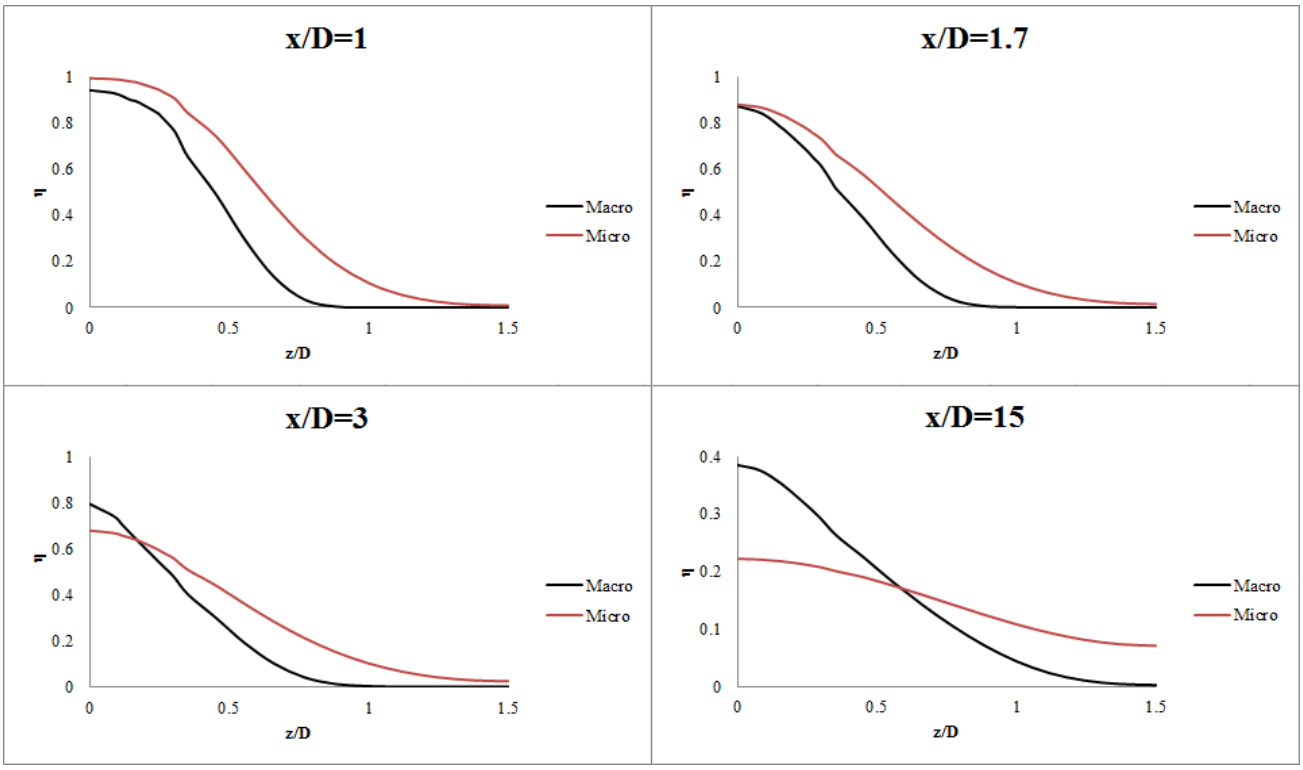


**Fig. 23 Lateral distribution of effectiveness for various x/D locations at M=0.5**

The lateral distribution of effectiveness shown in Fig.23 provides information about lateral distribution of coolant. The coolant from micro-hole spreads better in the lateral direction than the coolant from macro-hole. In vicinity region, the large momentum of the coolant form macro-holes lifts the jet away from the surface and lowers the performance. Conversely in the downstream region, the reattachment of the jet from macro-hole enhanced the effectiveness in the centerline but the stronger vortices from the macro-hole prevents the coolant to spread in the lateral direction whereas the low strength vortices from micro-hole results in better lateral distribution of the coolant.

Effectiveness plots at low blowing ratio in Fig.21 and Fig.22 shows that the flow penetrates deeper into the mainstream flow without break and spreads laterally in the downstream direction.

### 4.2.2 High Blowing Ratio (M=1)

At high blowing ratio the jet from the coolant hole lifts-off from the surface and provides low effectiveness. The temperature distribution for M=1 from macro-hole and micro-hole are shown in Fig.24

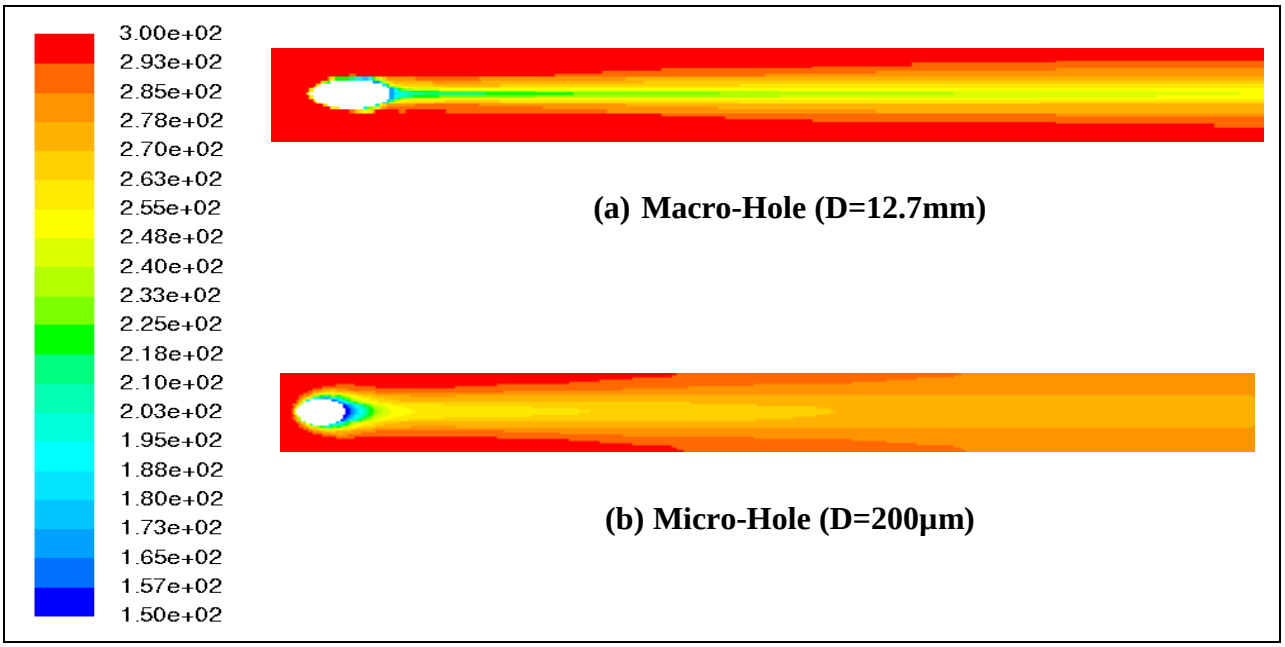


**Fig. 24 Temperature contour at M=1 for (a) macro-hole and (b) micro-hole**

The temperature distribution at high blowing ratio from macro-hole shows that coolant provides better cooling in the downstream region on the stream wise direction than the lateral direction. The high momentum of the coolant lifts the jet away from the surface and results in low performance at high blowing ratio. The jet from micro-hole dissipates quickly and provides better temperature distribution of coolant in the lateral direction as shown in Fig.24.

The jet from the micro-hole behaves better than the macro-hole in the vicinity region of x/D less than 3. The centerline adiabatic effectiveness in Fig.25 shows that the effectiveness from micro-hole decays faster than the macro-hole due to jet lift-off. In the downstream region effectiveness was increased for the macro-hole due to the reattachment of coolant jet in the downstream region, whereas the large L/D ratio for micro-hole prevents the reattachment of the jet and results in low performance in the downstream region for the coolant jet from micro-hole.

The laterally averaged effectiveness in Fig.26 shows that in vicinity region the micro-hole performs better than the macro-hole. For x/D greater than 3 due to the reattachment of the jet the macro-hole performs better than the micro-hole. Fig. 26 shows the averaged lateral distribution of the coolant from the hole, whereas the detailed information about the lateral distribution of coolant from the macro and micro-hole was recorded through the local effectiveness plot along the lateral direction as shown in Fig.27

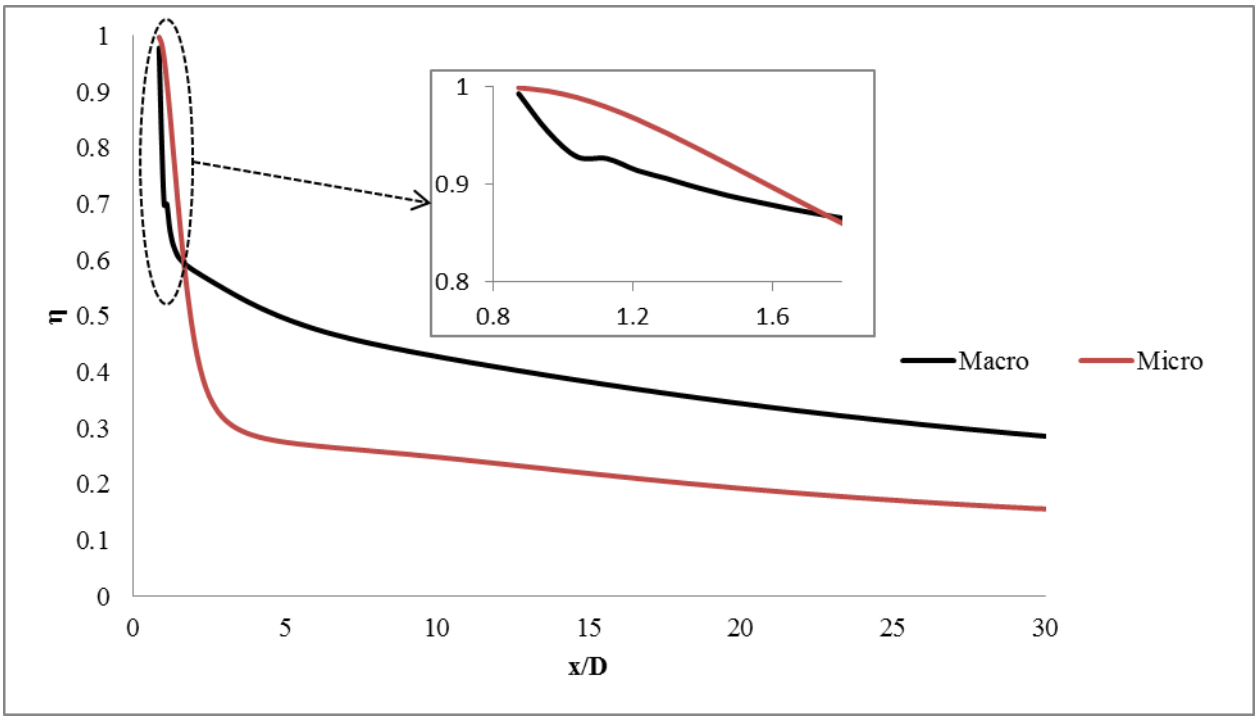


**Fig. 25 Comparison of centerline adiabatic effectiveness at M=1**

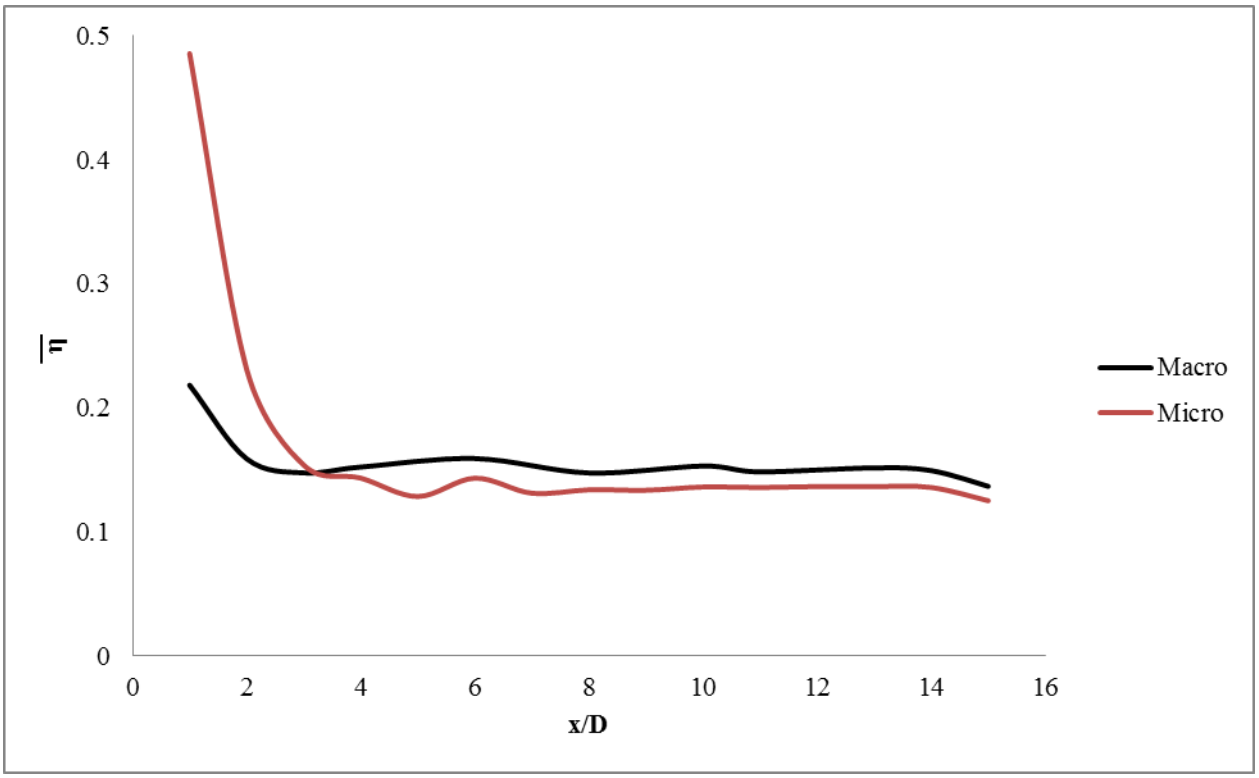


**Fig. 26 Comparison of laterally averaged effectiveness at M=1**

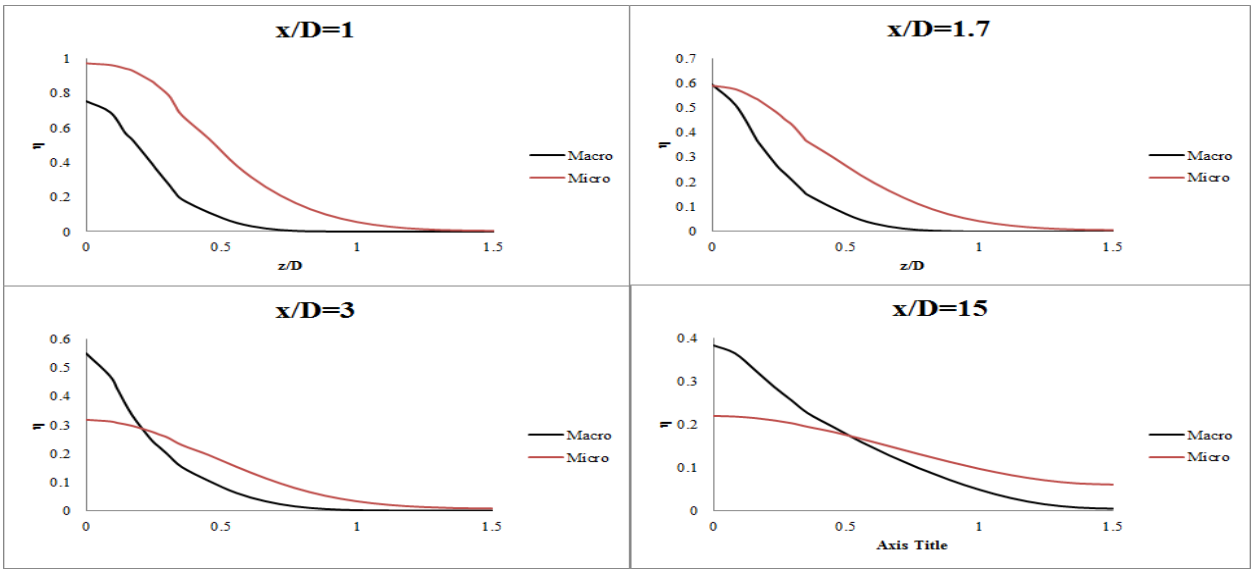


**Fig. 27 Lateral distribution of Effectiveness for various x/D locations at M=1**

The lateral distribution of effectiveness shows that in the region closer to the coolant hole, the coolant from macro-hole shows poor performance due to jet lift-off. At x/D of 3 and 15 the macro-hole behaves better than micro-hole in the centerline region but fails to spread laterally due to the greater strength of the vortices and momentum of the jet from macro-hole.

The coolant jet from micro-hole for both blowing ratio shows that the flow penetrates deeper in the mainstream without breaking and provides better lateral distribution of coolant. The jet reattachment was occurred in macro-hole which is absent for the jet from micro-hole due to large L/D ratio of the coolant hole. The micro-hole provides greater effectiveness in the vicinity region of the coolant hole due to decrease in momentum of the jet with respect to the mainstream flow as discussed above.

### 4.3 Flow Structure

From the effectiveness plot it was studied that flow from the micro-hole maintains its structure without a break and penetrates deeper into the mainstream flow without mixing. The coolant from macro-hole shows jet lift-off and reattachment in the downstream region due to high momentum of the jet and low L/D ratio of the coolant pipe. The high momentum jet injects into the mainstream flow generates vortices of high strength which pulls the hot mainstream flow towards the hot plate and results in lower performance. Unfamiliar physics of the flow structure of the micro-flow is analyzed and compared with the flow from the macro-hole.

### 4.3.1 Vortex Structure

Previous studies have registered that the counter rotating vortex pair (CRVP) is the primary reason for detachment of coolant jet from the surface. These vortices pull the hot mainstream flow towards the plate surface and entrain the surface with hot fluid results in low cooling performance. The effect of the CRVP for the coolant jet from macro-hole and micro-hole has been shown by overlaid velocity vectors on temperature contour as shown in Fig.28 and Fig.29. The overlaid velocity vector provides details about the vortex structure and the temperature contour shows the variation of coolant performance due to the CRVP. The information about the change in colours on the temperature contour is shown in the legends at the bottom of the figures.

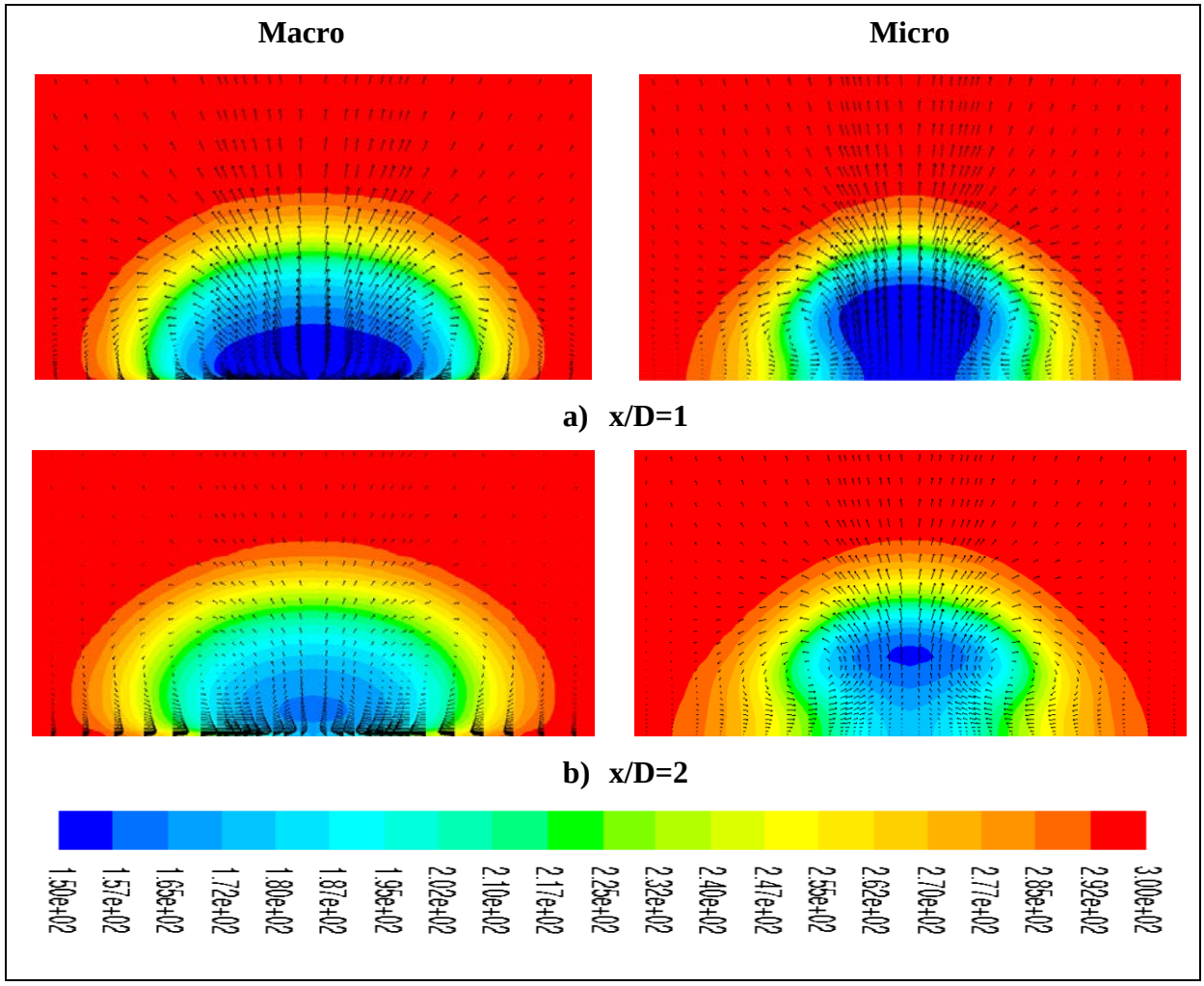


**Fig. 28 Flow structure from macro and micro-hole for M=0.5 at (a) x/D=1 and (b) x/D=2**

The effect of CRVP due to the low momentum jet at low blowing ratio (M=0.5) keeps the flow attached to the surface. A strong upwash was observed closer to the surface for the vortices from the macro-hole as shown in Fig.28 which prevents the coolant to spread in the lateral direction whereas the low strength vortices from micro-hole are smaller in size and move closer to each other which lower the upwash effect and allows the coolant to spread in the lateral direction. The strength of the CRVP is reduced in the downstream region of x/D=2 and the dissipation of the coolant is observed from the temperature contour shown.

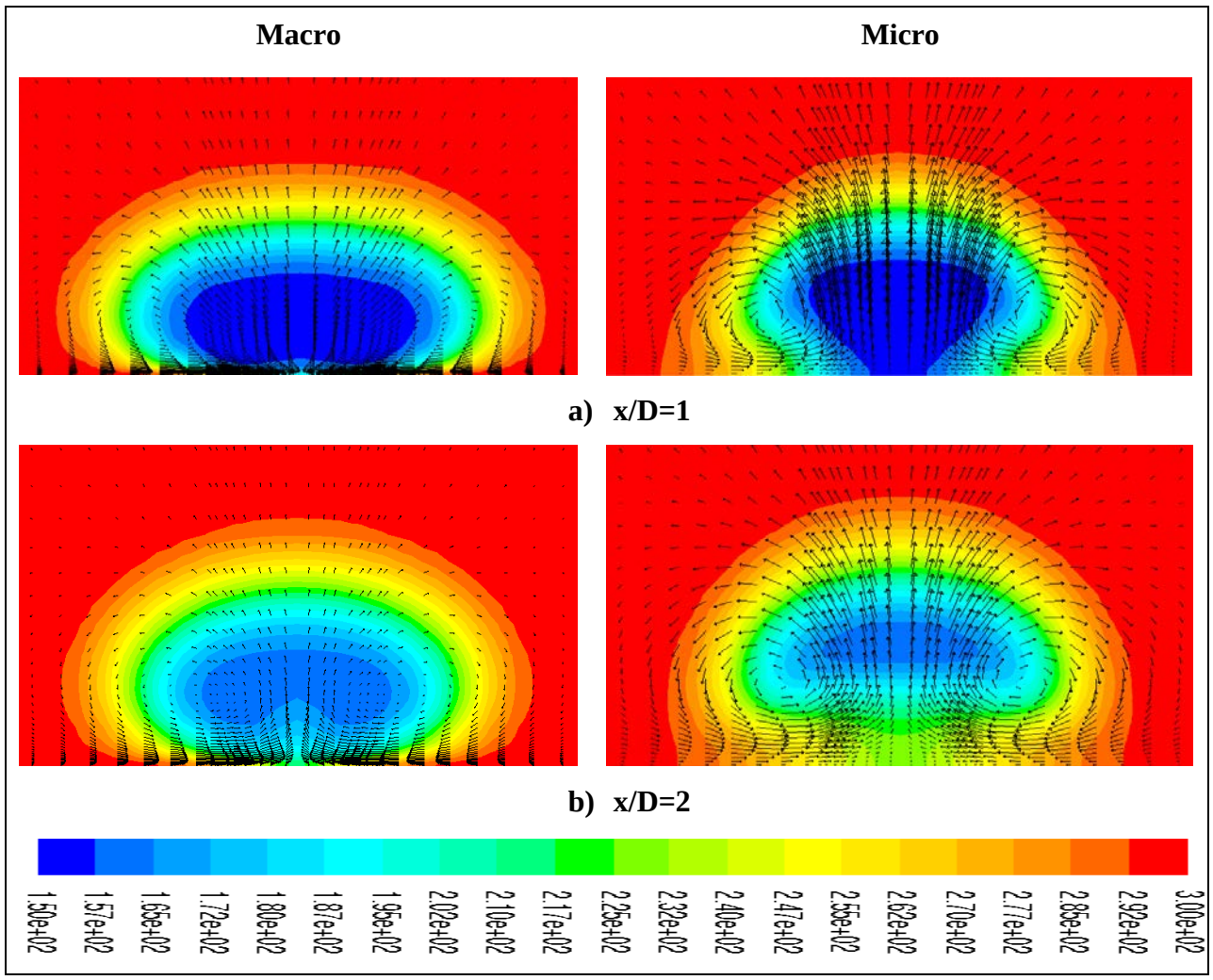


**Fig. 29 Flow structure from macro and micro-holes for M=1 at (a) x/D=1 and (b) x/D=2**

At high blowing ratio, large momentum of the jet increases the strength of vortices. The stronger vortices from the macro and micro-hole is shown in Fig.29, the strong upwash in macro-hole lifts the coolant away from the surface. The strong downwash in micro-hole reduces the effect of upwash close to the plate and keeps the coolant jet attached which dissipates quickly in

the lateral direction as shown in the temperature contour. In the downstream region the strength of the downwash gets weaker and the strong upwash lifts the jet away from the surface as shown.

The temperature contours for both blowing ratios in Fig.28 and Fig.29, show that the jet from micro-hole dissipates faster than the macro-hole due to the strong downwash on the CRVP of the coolant jet from the micro-hole. The coolant jet from macro-hole lifts away from the surface and then reattached in the downstream region, but the coolant from micro-hole lift away and dissipates laterally on the surface at both blowing ratio, which shows that the coolant from micro-hole maintain its structure without break. The strong dissipation is due to the strong downwash found in the jet from micro-hole with closer CRVP.

### 4.4 Multiple Micro-hole Film cooling

The extent computational study of film-cooling from two micro-holes with pitch distance of 3D (P/D=3) is carried out and performance of the multiple micro-holes is compared with the performance of discrete micro and macro-hole. The model and mesh for the multiple-hole geometry is created on GAMBIT in the same way as mentioned for the discrete holes in chapter-2 and chapter-3. The mesh with 2.6E5 nodes is found independent to the performance of multiple-holes, the boundary conditions and the operating conditions are similar to the simulation of discrete micro-hole as mentioned in chapter.3. The performance of multiple micro-hole film cooling is compared with the performance of discrete micro-hole and macro-hole film cooling in Fig.30

#### 4.4.1 Geometry

The geometry for multiple micro-holes simulation is based reference diameter of 200μm where the domain extends on the upstream and downstream region was similar to the geometry of the discrete hole. The L/D ratio was selected based on the analysis from Chapter-3 and the plenum was included in the study to involve the effects of velocity profile in coolant hole. The geometry of multiple micro-holes used for simulation is showed in Fig.30 where the P/D ratio of 3D is used based on the study of Sinha et al [9]. The small modification of P/D ratio of 3 was used along the stream wise direction whereas Sinha et al used the P/D ratio in lateral direction.

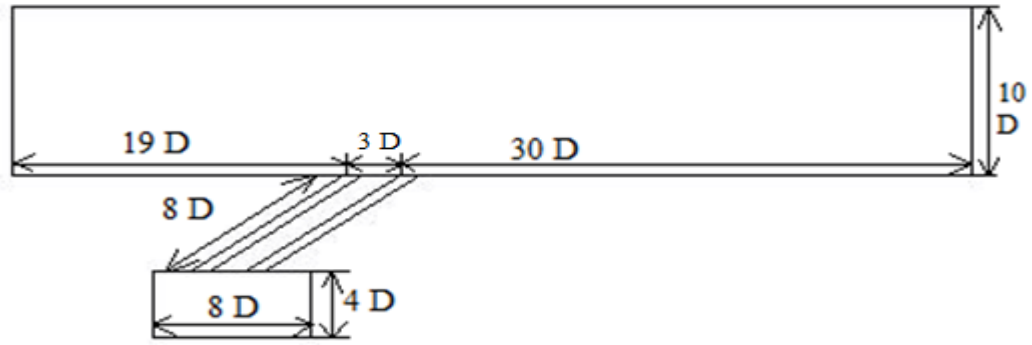


**Fig. 30 Geometry for multiple micro-holes simulation**

The operating conditions are same as the operating conditions used for discrete micro-hole and the performance of the coolant from multiple micro-holes is discussed in the following sections.

### 4.4.2 Performance of the multiple hole micro-film cooling

**a) Low Blowing Ratio**

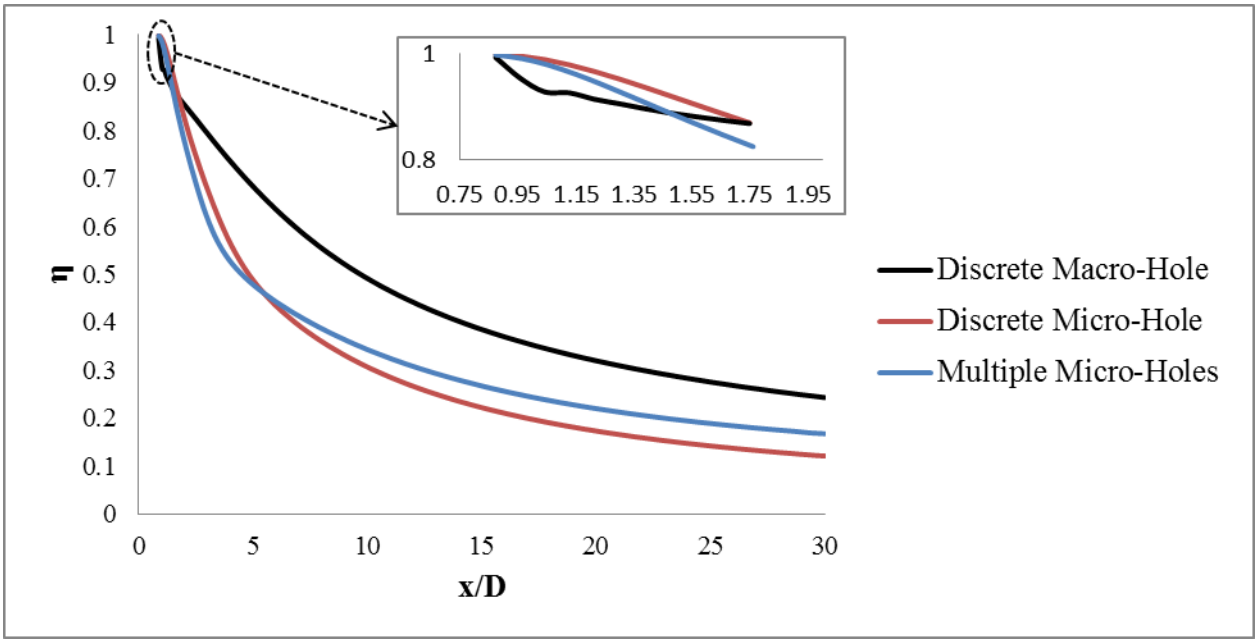


**Fig. 31 Centerline adiabatic effectiveness for multiple micro-holes and discrete micro and macro-holes at M=0.5**

The centerline adiabatic effectiveness for multiple micro-holes is calculated from the trailing edge of the second hole, the comparison was made between the performance of discrete micro-hole and macro-hole as shown in Fig.31. The centerline adiabatic effectiveness from the multiple hole shows the lower performance in vicinity region of x/D < 1.7 than discrete micro-

hole but in the region of 1.7 < x/D < 6 the rate of decay of effectiveness is higher for the multiple micro-holes than discrete holes and in downstream region of x/D > 6 the multiple-holes shows better performance than discrete micro-hole due to the jet reattachment.

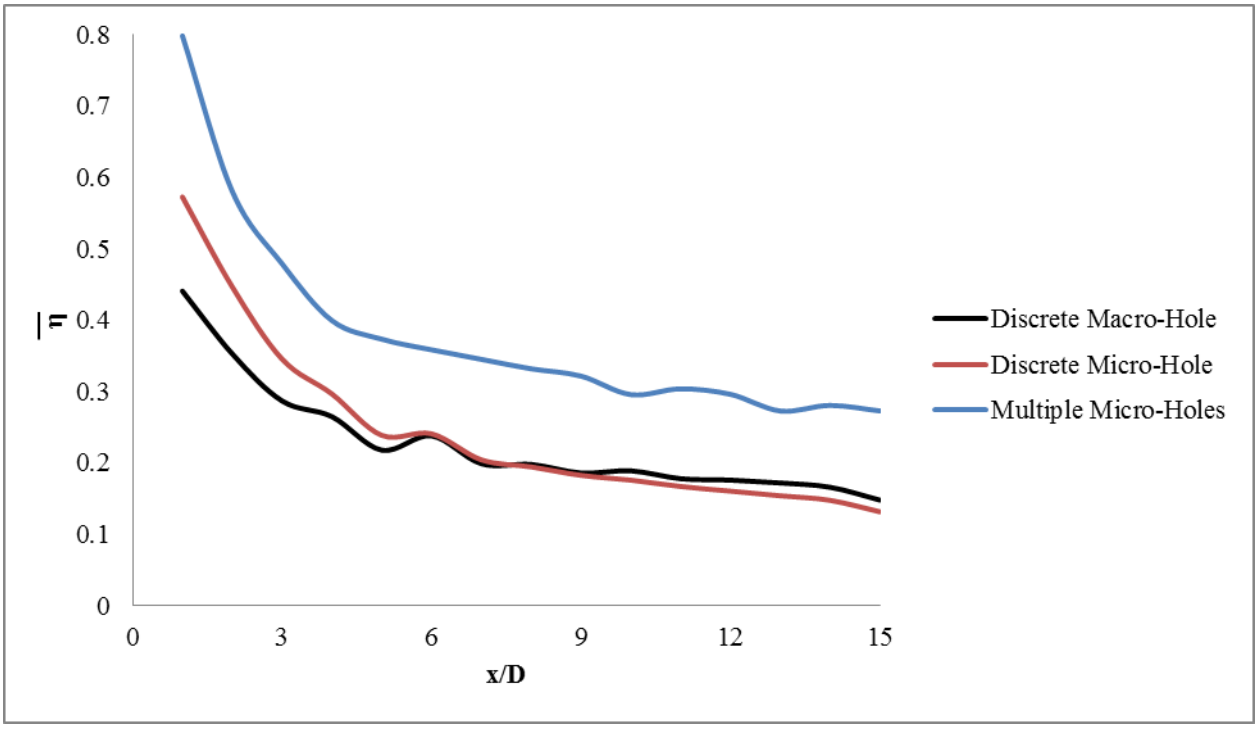


**Fig. 32 Laterally averaged effectiveness for multiple micro-holes and discrete micro and macro-holes at M=0.5**

Comparison of the laterally averaged effectiveness in Fig.32 shows that coolant from multiple micro-holes spreads tremendously in the lateral direction then discrete holes. This tremendous spreading of the coolant is due to increase in the amount of coolant than the discrete micro-hole, however the jet from the first hole interacts with the jet from second hole cause the jet to lift-off and reattached in the downstream region. The interaction of the jets increase the strength of the vortices and lift the jet away from the surface and reattached in the downstream region due to the decrease in vortex strength.

### c) High Blowing ratio

At high blowing ratio the centerline adiabatic effectiveness of the multiple micro-holes and discrete holes shown in Fig.33 were performed in a similar way as for low blowing ratio i.e. the jet from multiple micro-holes show jet lift off due to high momentum of the jet and reattached in the downstream region results in better effectiveness than the discrete micro-hole. Unfamiliar

flow physics for the coolant jet from the multiple micro-holes needs more detailed study of the flow structure.

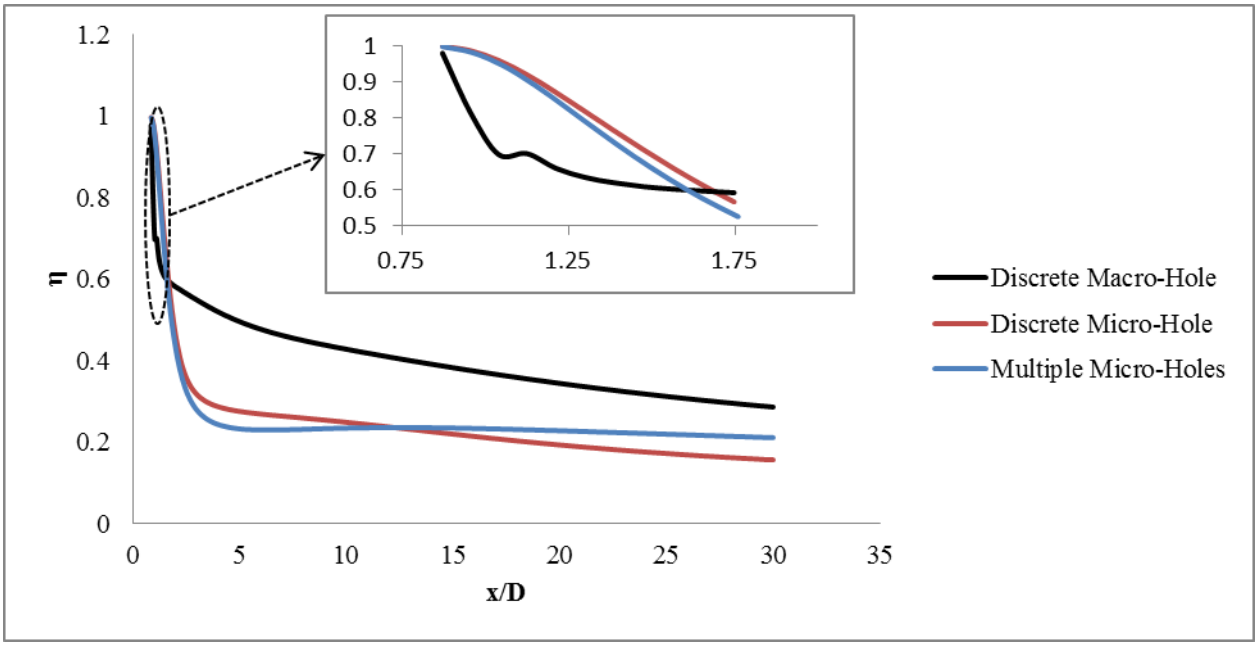


**Fig. 33 Centerline adiabatic effectiveness for multiple micro-holes and discrete micro and macro-holes at M=1**

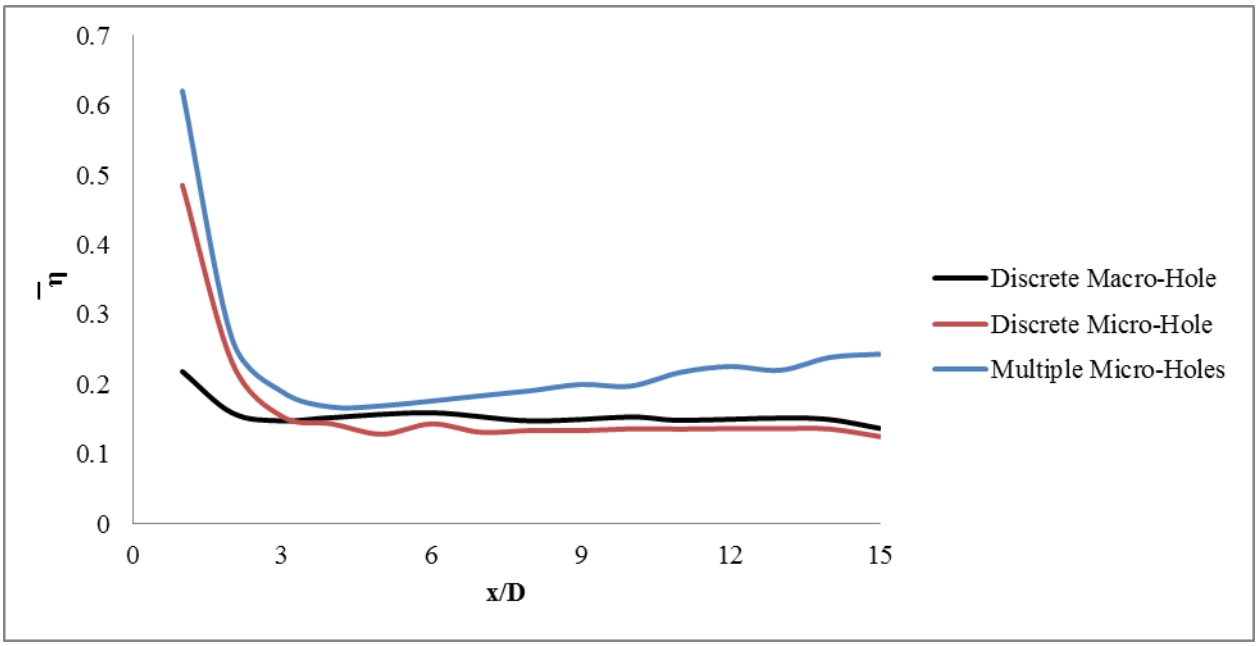


**Fig. 34 Laterally averaged effectiveness for multiple micro-holes and discrete micro and macro-holes at M=1**

The comparison of laterally averaged effectiveness in Fig.34 gives more detail information about the flow from multiple micro-holes. It was evident that at high blowing ratio the momentum of the jet from second hole is increased due to interaction of the high momentum jet from first hole which lifts the jet of the second hole away from the surface and reattached in downstream region as shown in Fig.34. The increase in amount of the coolant due to jet interaction for multiple micro hole results in better lateral distribution of coolant than discrete holes.

### 4.4.2 Flow Structure

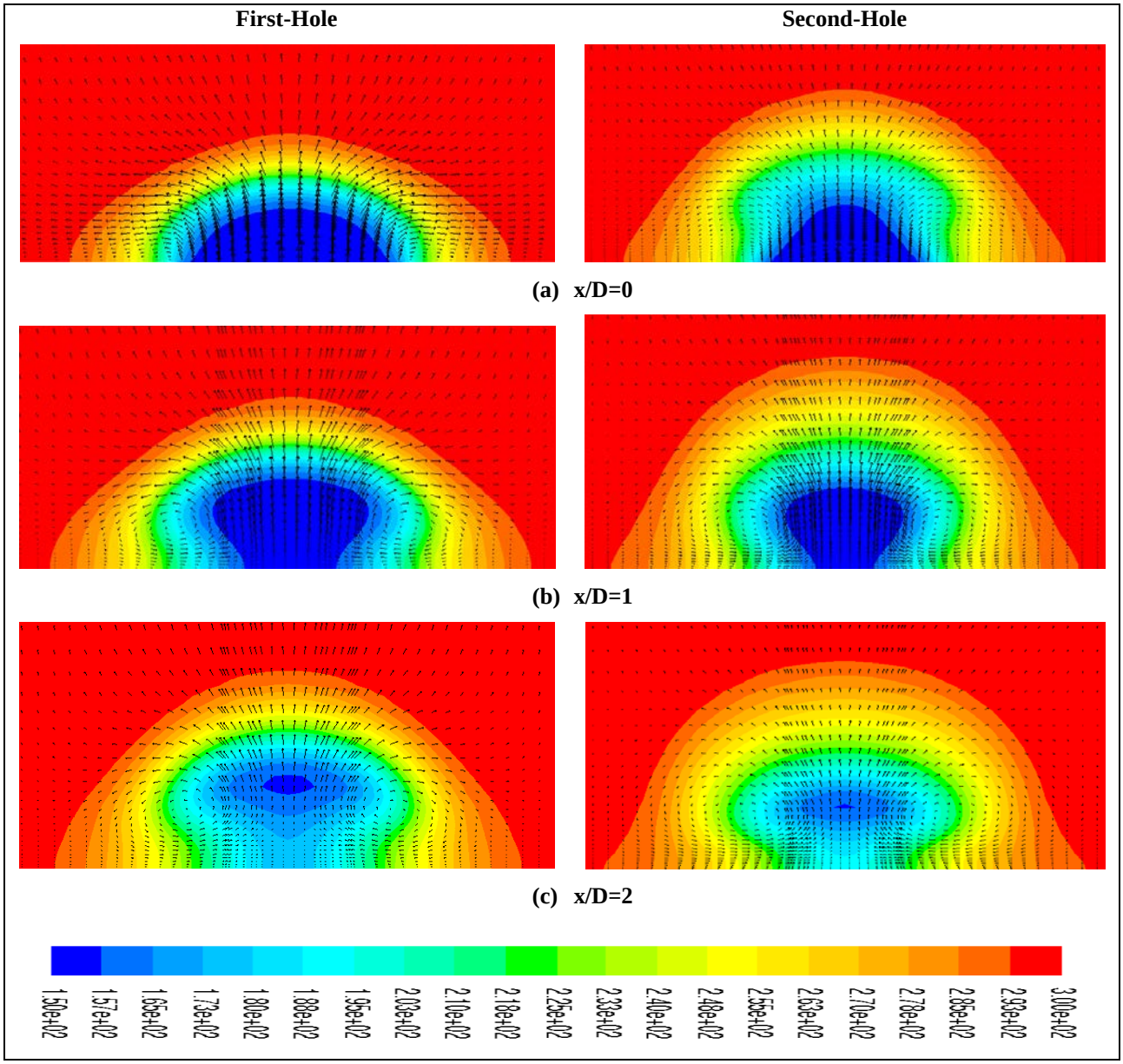


**Fig. 35 Flow structure from the first and second hole for M=0.5 at (a) x/D=0, (b) x/D=1 and (c) x/D=2**

The complex flow structure of the jet from the multiple holes is due to the interaction of the jets from the previous hole. The interaction of the jets increase the strength of the vortices from the second hole, results in jet lift-off away from the surface. The analysis of the vortex structure from the first hole and second hole for both blowing ratios give detailed information about the complex behaviour of the flow from the coolant holes.

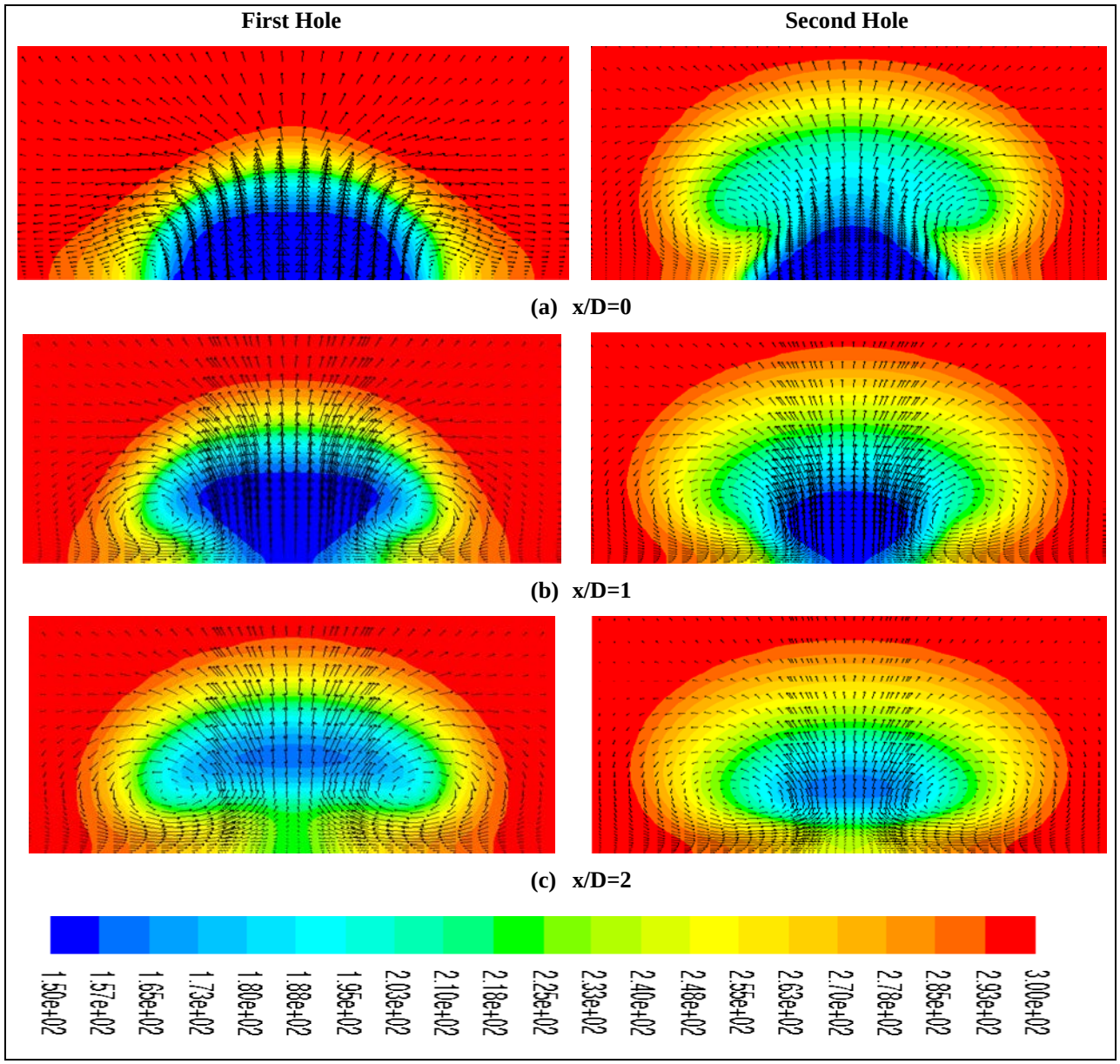


**Fig. 36 Flow structure from the first hole and second hole for M=1 at (a) x/D=0, (b) x/D=1 and (c)x/D=2**

The flow structure from the first hole and the second hole for a low blowing ratio of (M=0.5) is shown in Fig.35 at various locations of x/D from 0 to 2 whereas the second hole is positioned at P/D ratio of 3 from the first hole in stream wise direction. The flow from the first

hole behaves like a flow from the discrete hole as mentioned in section 4.3.1. The vortex from the first hole at x/D=2 interacts with the emerging flow from the second hole at x/D=0 creates a strong upwash of the coolant as shown in Fig.34. The vortices merge together in the downstream direction results in strong upwash for the flow from second hole at x/D=1 and 2 lifts the jet away from the surface and the downwash dissipates the coolant along the lateral direction as shown. The interaction of the vortices for coolant from multiple micro-holes increase the momentum of the coolant jet and lift the jet away from the surface and the momentum of the jet reduces in the downstream region results in the jet reattached in the downstream region.

The performance of coolant jet from multiple micro-holes shows the jet lift-off and reattached for both blowing ratios whereas the flow at jet exit from the discrete hole in section 3.3.2 the jet reattachment was not observed for both blowing ratios. The common observation is that the vortices from the first hole interact with the vortices form the second hole results in increase in momentum of the jet from the second hole and lifts the jet away from the surface. The CRVP from the first hole interacts with the emerging coolant from the second hole, which increases the strength of the CRVP and cause the jet to lift away from the surface. The jet lift off at low blowing ratio is found reattached earlier than the high blowing ratio coolant jet. The interaction of the coolant jet disturbed the exit velocity profile of the jet at coolant hole exit, whereas the jet reattachment was not observed for fully developed flow from the coolant exit as observed in chapter.3. Further investigation with varying P/D ratio is needed to make the flow attached to the surface and provide better performance.

# Chapter 5: Conclusion

## 5.1 Summary

Numerical Analysis for the performance of coolant jet from discrete and multiple micro-holes with plenum have been carried out in this study with a reference of the experimental results of Sinha et al [9]. The facts understood from this computational study with the highly refined grid are briefly discussed in this chapter. The performance of the coolant jet from macro and micro-hole are carried out for both discrete holes and multiple micro-holes. The vortex structure from macro and micro-holes are also captured and discussed.

### 5.1.1 Validation

Before starting the analysis of the coolant jet from micro-hole, the computational grid and the predicted results has been validated using the commercial FLUENT codes and was discussed in Chapter.2. The experimental study from Sinha et al [9] is used as a benchmark for the analysis of the coolant jet from micro-hole. The well-structured conformal quadrilateral grids have been created using GAMBIT and related momentum and energy equations have been solved using FLUENT-14 from High Performance Computing Virtual Laboratory (HPCVL), Queens University, ON, Canada. From the results it was found that the grid with 2.3E5 nodes is independent for the solution of the macro-hole film cooling performance.

Comparison between the performance prediction of SKE and RKE turbulence model has been made and found that the both models do not show much variation at low blowing ratio but at high blowing ratio the RKE model predicts the performance closer to the experimental results than the SKE model. So the RKE model with the numerical setup mentioned in section 2.4.3 and section 3.2.2 is used for analysis.

### 5.1.2 Micro-hole Geometry

` The application of micro-hole in the experimental model results in the large L/D ratio which requires large memory and computational time. In order to use the available computational resources in effective manner, the behaviour of micro-jet inside the coolant pipe for various L/D ratios have been studied before selecting the geometry for the analysis on micro-holes.

The study of flow behavior in the coolant pipe for various L/D ratios have been carried out and the results are discussed in chapter 3. At low L/D ratio the coolant jet found difficult to turn, detached from trailing edge of the coolant pipe and is accelerated towards leading edge of the coolant pipe. Finally it was concluded that at L/D ratio greater than 5 the jet becomes fully developed and a very little variation in the performance was observed between L/D ratio of 8 and 10 than the variation between L/D ratio of 5 and 8. For the effective use of available computational resources L/D of 8 was selected for analysis on Micro-hole.

### 5.1.3 Comparative Study

The comparison between the performance of the coolant jet from macro and micro-holes have been studied. The effectiveness of the micro-hole is found superior to the macro-hole in the vicinity region and also found that the local distribution of the effectiveness in the lateral direction is better for the micro-hole than the macro-hole. The jet from micro-hole does not show reattachment in the downstream region due to the large L/D ratio for micro-hole. The vortex structure is also captured and found that the decrease in jet diameter makes the counter rotating vortices to move closer as well as the strong downwash cause the coolant to spread laterally. The low strength vortices results in the coolant to dissipate in lateral direction and low performance in the downstream region.

The performance from the multiple micro-holes coolant jet is also simulated and compared with the performance from the discrete macro and micro-holes. The jet lift-off and reattachment was found for the jet form second hole due to the interactions of the coolant jet from the first hole with coolant jet from second hole. This jet interaction disturb the exit velocity profile of the jet from the second hole and cause the coolant to lift off and reattached in the downstream direction. But the jet lateral distribution was extremely increased due to the increase in mass flow rate of the coolant than discrete micro-hole. The P/D ratio used for multiple hole was based on the P/D ratio for macro-hole used by Sinha et al [9], thus for micro-hole study further analysis on P/D ratio is required.

The other common observation found from the performance of the coolant from macro-hole and micro-hole film cooling is listed below.

- The reduction in coolant area decreases the amount of bleed air from the compressor which is used as a coolant for film cooling.
- The reduction in bleed air increases the engine performance by the use of small amount of fuel.
- The decrease in coolant area lowers the momentum of the coolant jet from micro-holes.
- The decreases in the area move the counter rotating vortices closer to each other and lower the strength.
- The application of micro-hole in the experimental setup increases the L/D ratio allows the coolant jet fully developed before exit to the mainstream region.

### 5.5 Future Works

The above analysis is a basic study of micro-hole film cooling and further studies are required to explore and understand the performance of micro-hole film cooling. Some of the future studies in micro-hole film cooling are recommended as follows

- The RKE model captures the complex flow structure better than the SKE model but the improvement is not clear, so the DNS/LES turbulence model would be used in future analysis.
- Conduct a study on any one of the major disadvantages in the application of micro-hole, for instance the coolant hole “blockage” due to the debris in the mainstream flow
- A detailed study on the variation of P/D ratio (lateral and stream wise direction) for micro-hole film cooling without affecting the aerodynamic characteristics of the flow in gas turbine vane.
- A detailed CFD study of the application of micro-hole for film cooling on turbine vane leading edge to increase the cooling performance which was proved experimentally by Sriram and Jagadeesh[13] for the blunt body.

The above suggested investigations are only few works for future reference. However still more work could be made computationally and experimentally. As mentioned before researchers are working for more than six decades in this massive field to increase the performance of film cooling.

**References**

[1] Je-Chin Han, Sandip Dutta and Srinath V.Ekkad, 2000 *"Gas Turbine Heat Transfer and Cooling Technology"*, Taylor and Francis Publications.

[2] Bogard.D.G and Thole.K.A, 2006 *"Gas Turbine Film Cooling*", Journal of Propulsion and Power vol.22, No.2. pp. 249-270

[3] Thole.K.A, Gritsch.M, Schulz.A and Wittig.S, 1997 *"Effect of a Crossflow at the Entrance to a Film_Cooling Hole"*, Journal of Fluids Engineering, vol.119, pp. 533-540

[4] J. Andreopoulos and Rodi.W, 1984 *"Experimental investigation of jets in a crossflow"*, Journal of Fluid Mechanics, vol.138, pp 93-127

[5] Jue Zhou and Shan Zhong, 2009, *"Numerical simulation of the interaction of a circular synthetic jet with a boundary layer"*, Journal of computers and Fluids, vol 38, pp-393-405

[6] Fric.T.F and Roshko.A, 1994, *"Vortical structure in the wake of a transverse jet"*, Journal of Fluid Mechanics, vol.279, pp 1-47

[7] Walters.D.K and Leylek.J.H, 1997, *"A Systematic Computational Methodology Applied to a Three-Dimensional Film Cooling Flowfield"*, Journal of Turbomachinery, vol.119, pp-777-785

[8] Walters.D.K and Leylek.J.H 2000, *"A Detailed Analysis of Film Cooling Physics: Part I-Streamwise Injection with cylindrical Holes"*, Journal of Turbomachinery, vol.122, pp-102-112

[9] Sinha.A.K , Bogard.D.G and Crawford.M.E 1991, *"Film-Cooling Effectiveness Downstream of a Single Row of Holes with Variable Density Ratio"*, Journal of Turbomachinery , vol.113, pp-442-449

[10] Azzi.A and Jubran.B.A, 2003, *"Numerical Modelling of Film Cooling from Short Length Stream-Wise Injection Holes"*, Heat and Mass Transfer, vol.39, pp-345-353.

[11] Azzi.A and Jubran.B.A, 2007, *"Numerical Modelling of Film Cooling from Converging slot-hole"*, Heat and Mass Transfer, vol 43, pp-381-388

[12] Asghar.F.H and Hyder.M.J, 2011, *"Computational study of film cooling from single and two staggered rows of novel semi-circular holes including coolant plenum"*, Journal of Energy conversion and Management, vol.52, pp-329-334

[13] Sriram.R and Jagadeesh.G, 2009, *"Film cooling at Hypersonic Mach Numbers forward facing array of Micro jets"*, International Journal of Heat and Mass Transfer, vol.52, pp-3654-3664

[14] Li.P.L, Ko.H.S, Jeng.D.Z, Liu.C.W and Gau.C, 2009, *"Micro Film Cooling Performance"*, International Journal of Heat and Mass transfer52, pp-5889-5894

[15] Ferguson.J.D, Walters.D.K, and Leylek.J.H, 1998, *"Performance of Turbulence Models and Near-wall Treatments in Discrete Jet Film Cooling Simulations"*, ASME, 98-GT-438

[16] Na.S, Zhu.B, Bryden.M and Shih.T.I.P, 2006, *"CFD Analysis of Film Cooling"*, 44th AIAA Aerospace Science Meeting and Exhibit, AIAA 2006-22

[17] Marc.J.Ely and Jubran.B.A, 2009, *"A Numerical evaluation on the effect of sister holes on film cooling effectiveness and the surrounding flow field"*, Heat and Mass transfer. Vol.45, pp-1435-1446

[18] Marc.J.Ely and Jubran.B.A, 2009, *"A Numerical Study on Improving Large Angle Film Cooling Performance through the use of Sister Holes"*, Numerical Heat Transfer, Part-A, An International Journal of Computation and Methodology. vol.55, pp-634-653.

[19] Rajappan.R, and Mahalakshmi.N.V (2011), *"Computational study of free-strem Turbulence effects using two different models"*, Progree in Computational Fluid Dynamics, Vol.11, No.2, pp-96-104

[20] Goldstein.R.J, Eckert.E.R.G and Ramsey.J.W (1968), *"Film Cooling with injection through a circular Hole"* NASA CR-54604

[21] Hassan.O and Hassan.I (2013), *"Experimental investigations of the film cooling effectiveness of a micro-tangent-jet scheme on a gas turbine vane"*, International Journal of Heat and Mass Transfer 61, pp-158-171

[22] Phil Ligrani, Matt Goodro, Mike Fox and Hee-Koo Moon (2013), *"Full-coverage Film Cooling: Film Effectiveness and Heat Transfer Coefficients for dense Hole Arrays at different Hole Angles, Contraction Ratios and Blowing Ratios"*, Journal of Heat Transfer 135(3),031707

[23] Jack L.Kerrebrock (1978), *"Aircraft Engines and Gas Turbines"*-second edition, The Alpine Press Inc.

## Appendix

1. Multiple-Hole Film cooling performance

   i. Temperature Contour

      a) Low blowing ratio (M=0.5)

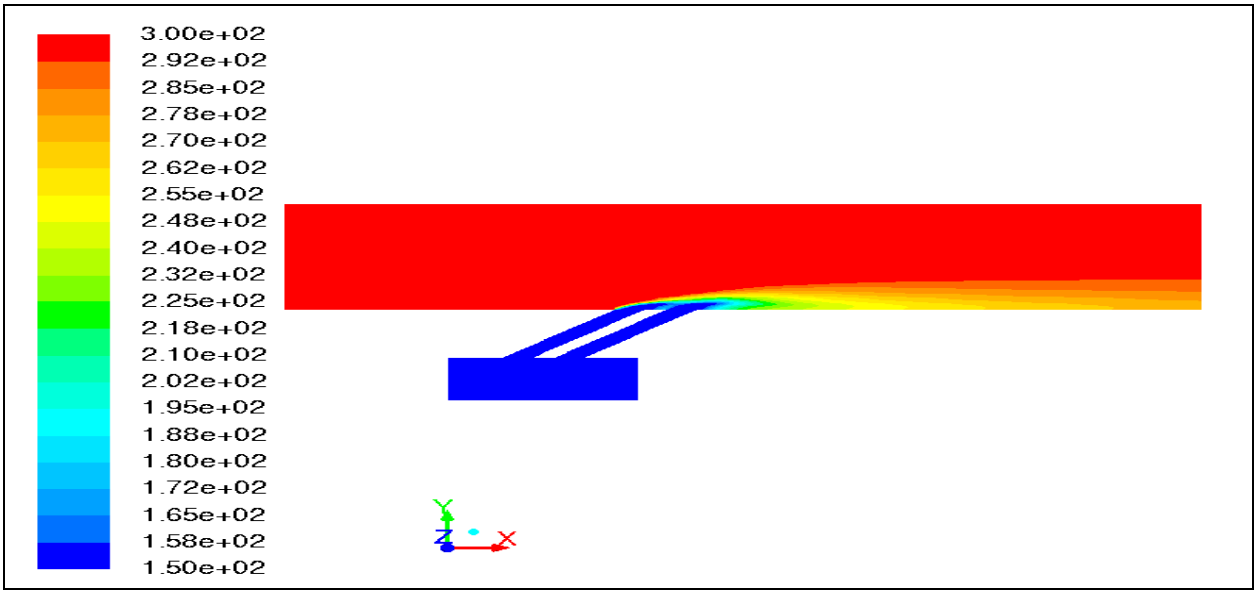


**Fig. 37 Temperature contour for multiple micro-holes in the mid-plane at z=0 for M=0.5**

      b) High blowing ratio (M=1)

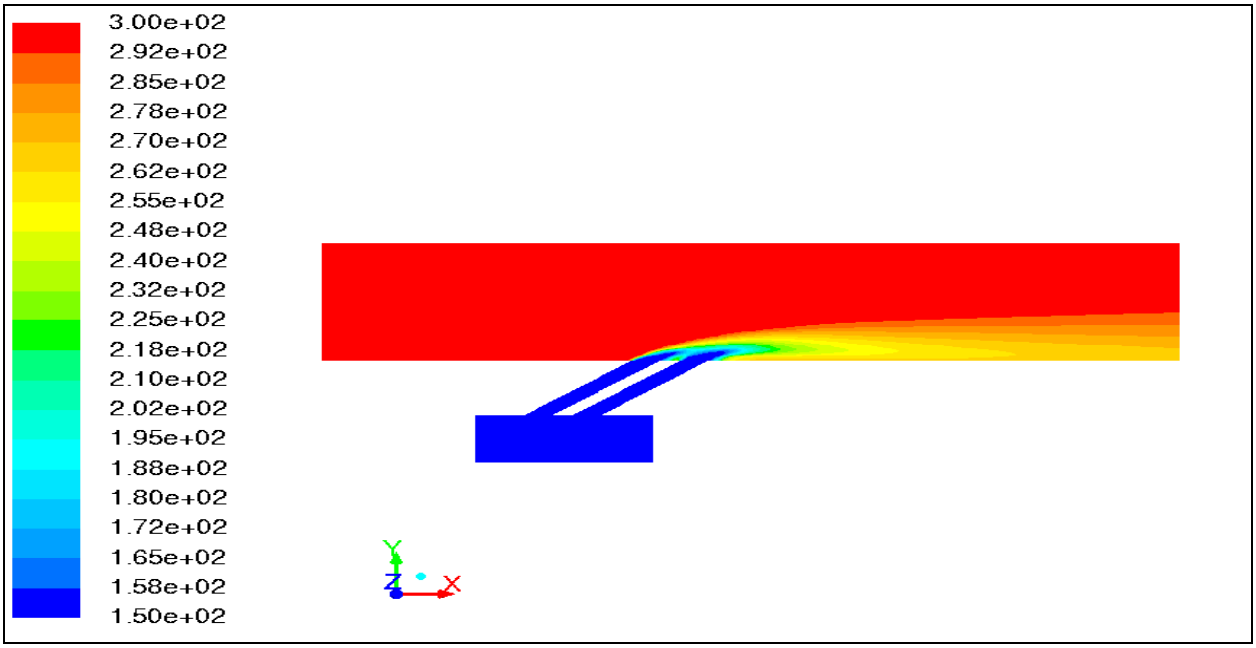


**Fig. 38 Temperature contour for multiple micro-holes in the mid-plane at z=0 for M=1**

2. Lateral Temperature Distribution in Multiple Hole

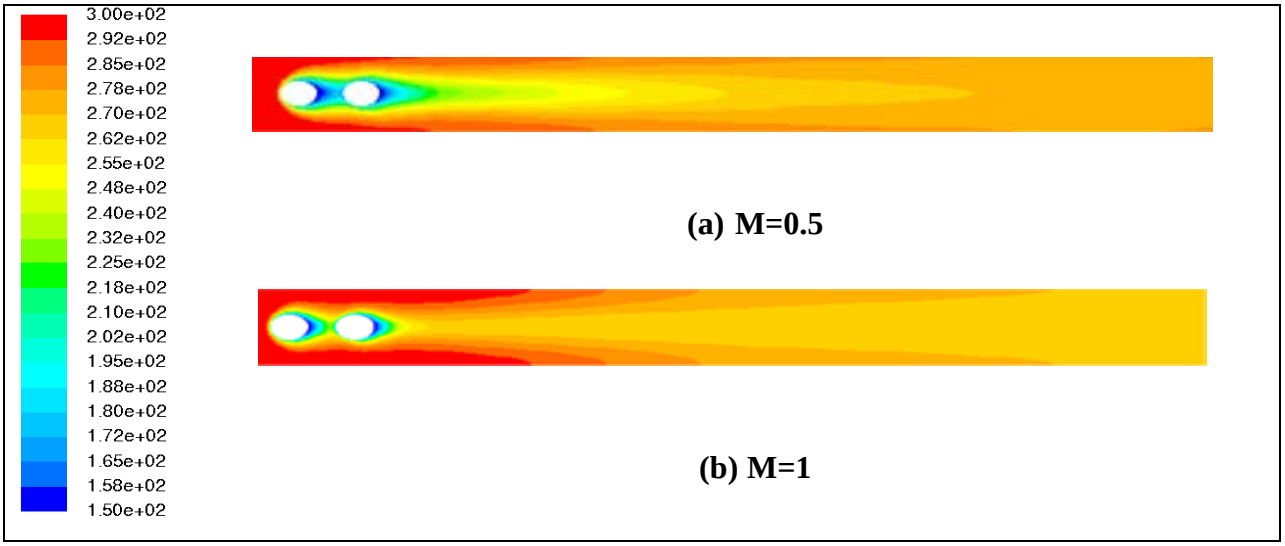


**Fig. 39 Temperature distribution from multiple holes for (a) M=0.5 and (b) M=1**